A COMPARISON OF THE STRESSES IN THE CRANKSHAFT OF AN INTERNAL COMBUSTION ENGINE AS DETERMINED BY USING ELECTRICAL RESISTANCE STRAIN GAGES AND BY ANALYTICAL METHODS

by

Billy Yick-Kwan Mui

Thesis submitted to the Graduate Faculty of the
Virginia Polytechnic Institute
in candidacy for the degree of
MASTER OF SCIENCE
in
MECHANICAL ENGINEERING

TABLE OF CONTENTS

Page

LIST OF FIGURES

Page

I. INTRODUCTION

The goal of modern internal combustion engine designers is to develop a light-weight, high performance, but inexpensive engine. To reach this goal a very accurate estimation of the stresses in the engine members is required.

A factor of safety has been applied to design works since the development of the art of analytical stress analysis. A large factor of safety is used if little information about the actual working stresses in the machine member to be designed is known. Therefore an optimum design cannot be reached unless the actual stresses are known. The experimental stress analysis is developed in order to determine the actual working stresses in a machine member. However, the experimental determination of the stress cannot be carried out until the machine member is designed and made. If a comparison between the stresses obtained by analytical method and by experimental method is made, the comparison can be used in return, to improve the new design.

In the 1958 winter quarter, the writer took a crankshaft design subject in the course, Internal Combustion Engine Design, instructed by Professor C, E. Trent of the Mechanical Engineering Department at the Virginia Polytechnic Institute. The writer became interested at that time in finding out what the actual stress would be if the designed

crankshaft were put into operation. The idea was then carried out and became the subject of this thesis.

Several experimental methods for determining stresses in a machine member have been developed and applied successfully. One of these methods utilizes electrical resistance strain gages. The electrical resistance strain gage is particularly useful in stress alalysis work on an engine because of its negligible weight and size. The strain gage may be applied to parts which would be inaccessible with other gages, and senses the strain directly without any appreciable influence on the stress in the engine member.

Experimental stress analyses have been made on crankshaft of internal combustion engines by previous investigators, but no comparison to analytical results was found in the writer's review of literature. It was, therefore, decided to make such a comparison.

II REVIEW OF LITERATURE

The work done by previous investigators gives an invaluable guidance to later investigators. The literature review offered the writer a foundation and direction in which to carry out his investigation for this thesis. It is summarized below:

A. Experimental methods for determining stresses in the crankshaft of an internal combustion engine ---- Since stress is the force per unit area in a body, stress itself is not a quantity which can be measured directly. However, Hook's Law provides that within the elastic limit of a certain material the deformation of a body is proportional to the force acting on it, that is, the stress in a body is proportional to the strain of the body. Thus, the methods of measuring strains can be applied to determine stresses.

The methods of measuring strains as classified by Mr. B. F. Langer of the Westinghouse Electric Company included the following:

Mechanical

(1) direct

(2) brittle lacquer

(3) scratch gage

(4) pneumatic

(5) mechanical multiplication

Optical

(1) microscope

(2) mirror

(3) slit or grating

(4) polarized light

(5) photography

Electrical

(1) resistance

(2) inductance

(3) capacitance

(4) piezo-electric effect

(5) voltage generation

(6) vacuum tube with movable element

Each of the above methods is best suited for a particular fields of application. The method that should be chosen depends on the object to be investigated. However, " The electric resistance strain gage is a very valuable and powerful tool for measurement in that it not only enables measurements to be made in inaccessible places but also effects to the minimum quantity being measured. "[2]

Experimental determination of the stresses in the crankshaft of an internal combustion engine has been carried out by many investigators. One of these investigations made on

the crankshaft of a Wright R-1826-73 aircraft engine was carried out by Mr. Douglas P. Walstrom at the N.A.C.A. Cleveland Laboratory.[3] In this investigation Bakelite bonded wire strain gages made of Iso-elastic wire and Advance wire were installed on the front half of the crankshaft, and the connecting wires were brought out through the oil passages and connected to slip-rings at the rear of the engine. A Wheatstone-bridge and a 12 channel moving coil oscillograph were used as recording devices. Strains were measured while the engine was driven by the dymamometer through a range of speeds, and also with the engine operating under its own power through a range of speeds and powers. The following remarks are quoted from the report:

" Bonded wire strain gages applied to the accessible parts of the operating crankshaft make possible the following:

(1) measurement of actual peak stress

(2) separation of stresses into bending, torsional, and tensile stresses.

(3) analysis of the force applied to the crankshaft".[3]

In another investigation on the effect of torsional vibration, the Torsional Vibration Committee of the SAE War Engineering Board[4] used electrical resistance strain gages to measure the actual stresses in the crankshaft of a six cylinder internal combustion engine. SR-4 strain gages

were attached to the crankshaft by Dupont or Bakelite cement at the crankweb, crank pin, and fillets. The leads of the gages were taken out from the rotating shaft through oil holes. By means of slip-rings and brushes the gage output was transmitted to the instruments. The Wheatstone-bridge was used, and the signals from the strain gages were amplified by a R.C.A. amplifier, displayed on a 5 inch screen Dumont cathode-ray oscilloscope, and recorded by a camera.

B. The development of electrical resistance strain gages --- It may be interesting to note that carbon was the first kind of material used for electrical resistance strain gages. Mr. Claude M. Hathaway in a paper[5] gave the following statement on the development of the strain gage.

" In 1935 Mr. Hull of the General Electric Company invented the carbon-strip resistance gage, which he made by painting a small strip of paper with India ink. He found that if this strip were cemented to a member in which strain was to be measured, he could measure the strain by measuring variations in resistance of the strip. This gage was used successfully by Hull in measuring strain concentrations in fillets on steam turbine shafts. ..... While reading F. W. Bridgman's book on the physics of high pressure, the author's attention was called to the strain-resistance characteristics of certain metals, and this lead to an at-

tempt to measure strain by cementing a fine filament or wire grid to the member under test. This was done in 1937 and the experiment had practical possibilities, but that considerable development work would be necessary to obtain electronic equipment of sufficient sensitivity and stability to render this type of gage practical for general use ".

The development of the metallic wire resistance strain gage was contributed by many investigators and companies, but the Baldwin-Lina-Hamilton Corporation holds all patents on the manufacture and application of the bonded electrical resistance strain gages in the United States. [6] The first two commercial strain gages were built about June, 1939.

C. The selection of strain gages --- The factors that should be considered in choosing the proper strain gage as given by Mr. John Tarbox[8] included the following:

(1) Area of measurement
(2) Stress amplitude
(3) Complexity of stress
(4) Strain frequency
(5) Thermal conductivity of the member to be measured
(6) Temperature range
(7) Temperature change
(8) Humidity

Item (1) determines the required size of the gage; item (2) determines the required gage factor; item (3) determines the arrangement of the wire gird; and items (4) to (8) determine the material of the wire.

D. Methods of maintaining electrical contact --- A means of communication between the strain gages and the instruments recording the strain is necessary when resistance wire strain gages are used to measure strains. Slip-rings and brushes, or some other types of sliding contact are most commonly used as such a means of communication for measuring dynamic strain on a rotating member.

An investigation on the performance of slip-ring and brush systems for use in determining actual operating stresses in a rotating shaft system have been made by Francis J. Dutee, Franklyn W. Phillips, and Richard H. Kemp at the N.A.C.A., Cleveland Laboratory.[9] The following statements are quoted from their report.

" Test results of the slip-ring and brush combinations rated as the most practicble for use in circuits to measure dynamic strain are as follows:

(1) Plate-brass slip-rings and silver-graphite brushes

(2) Monel-metal slip-ring and silver-graphite brushes

(3) Shim-brass slip-rings and silver graphite brushes

(4) Inconel slip-ring and silver graphite brushes

(5) Silver-plated slip-ring and soft carbon brushes."

" The results of these tests were utilized in the design of a slip-ring and brush system that performed satisfactorily in a crankshaft and connecting-rod stress measuring application."

" A good slip-ring system for measuring dynamic strains can have an appreciable voltage drop, but it is important that the drop remain constant within very close limits."

" It should be noted that the ratio of slip-ring and brush interference to strain-gage signal varied inversely as the gage resistance, the gage strain-sensitivity factor, and range of strain at the point where the gage is mounted. This same ratio is not affected by changes in gage current. An improvement in the performance of a slip-ring and brush system can thus be effected by increasing the gage resistance, gage factor, and range of strain ".

E. Analytical methods of determining stresses in a crankshaft --- Various methods, theories and formulas have been developed to solve problems involving stresses and strains in machine members. These methods and formulas have been presented by many authors in text-books, papers, and lectures, and can by used to compute the stresses and strains in a crankshaft. However, because of the complicated nature of the strains imposed upon a crankshaft, an exact stress analysis is impractical.

Certain assumptions, approximations, and idealized conditions are made to solve the stress problems in crankshaft design. For instance, the load on a sleeve bearing is either considered to be a concentrated load at the center of the bearing, or considered to be a uniformly distributed load over the entire length of the bearing; the stresses on crankwebs, crankpins, journals, etc., are computed by analysing the loads at a portion of the crankshaft instead of taking the whole shaft and analysing all the loads simultaneously. Therefore ,the analytical determination of the stresses in crankshafts is an approximation. But since the analytical method is necessary for the purpose of design, how close the analytical method can predict the actual stress is important.

In his review of literature, the writer found that no comparison between the analytical determination of crankshaft stresses and experimental determination of crankshaft stresses has been made. It is probably because the complicated features of a crankshaft system and the complexity of the loading conditions make it impossible to apply one analytical method to all kinds of shafts.

F. The effect of vibration on crankshaft stresses --- There are two distinct kinds of vibrations that are present in a reciprocating engine:

(1) Vibration due to the engine as a whole because of

the unbalanced forces of its moving parts.

(2) Vibration due to deflections and distortions in the material of the component parts of the engine.

As far as crankshaft vibrations are concerned, torsional vibration is the main thing that should be considered. Many failures of crankshaft have been traced to abnormal vibration at critical speeds. As mentioned by Mr. J. Ormondroyd in 1931 in a paper,[10] " Engineers are creating more powerful internal combustion engines by increasing operating speeds. At the same time, and partly because of this, the ratio of weight to power is being make smaller and smaller. These two tendencies have emphasized the problem of torsional critical speeds in this type of prime mover. Today, there are few internal combustion engine systems which do not have at least one dangerous or annoying torsional critical speed in the running range." Therefore,the determination of critical speed as well as the determination of the crankshaft stress induced at resonance are important to crankshaft design.

However, because of the complicated features of the crankshaft, no mathematical method can be applied to evaluate the effect of vibration unless the shaft is reduced to an equivalent system. The type of an equivalent system is dependent on the system being considered. There are three types of equivalent system which can be applied with satis-

factory results:

(1) Concentrated-mass system --- The equivalent system is obtained by considering the moving masses at each cylinder and other large compact parts as concentrated masses connected by elastic shafts having no mass.

(2) Uniform-shaft system --- The equivalent system is obtained by averaging the various masses distributed along the shaft of the installation into a number of connected uniform shafts having both mass and elasticity.

(3) Combination equivalent system --- The equivalent system is one which uses any combination of concentrated masses and elastic shafts with mass.

When the inertia force, the stiffness factors and the damping factors of the actual system are known and the actual system is reduced to an equivalent system, the following quantities can be computed:

(1) The natural frequencies of torsional vibration.

(2) The peak amplitudes or stresses at synchronism between the natural frequencies of the torsional vibration and the disturbing torque impulses.

(3) The forced vibration amplitudes or stresses at various frequencies of the disturbing impulses.

The following methods can be used to calculate the stresses induced by torsional vibration:

(1) Solve directly the differential equations set up

for the system.

(2) Holzer table

(3) Lewis polar diagram

(4) Vector method

(5) Mobility method

(6) Electrical analogy of mechanical system

The natural frequency and undamped forced vibration calculations for concentrated mass equivalent systems are usually carried out by using a Holzer table, while the solution for the uniform-shaft equivalent system may be carried out graphically by using Lewis polar diagram.

The peak amplitude of torsional deflection when the crankshaft system is at resonance depends on the damping factors and the impulse forces. Operation at a critical speed results in deflections due to free vibration adding to the deflections from the exciting torque impulses until internal friction in the shaft material and the external friction such as that in the shaft bearings and that due to the piston thrust, will consume the equivalent of these torque impulses and the growth of the deflections will stop, thus reaching their maximum.

An investigation on the effect of torsional vibration of an internal combustion engine crankshaft has been carried out by the Torsional Vibration Committee of the SAE War Engineering Board for the use of the U. S. Navy. The

following remark is quoted from the report of the investigation.

" The strain and stress values thus obtained (by experimental methods) check well with the stresses calculated on the base of horsepower delivered and the rpm. In a readily calculable system, vibratory stress values obtained by using the magnetic pick-up agree reasonably well with the stresses obtained by means of strain gages".[12]

III THE INVESTIGATION

A. Object of the Investigation

The object of the investigation was to compare the stresses in the crankshaft of an internal combustion engine as determined analytically and experimentally in order to study the degree of accuracy with which the analytical methods used in the crankshaft design would predict the actual operating stresses in the crankshaft.

The two methods for determining crankshaft stresses -- namely, the analytical method and the experimental method, were compared by a set of curves using the following coordinates:

(1) Stress versus angular position of the crankshaft.

(2) Peak stress versus engine speed.

B. Method of Procedure

The investigation was divided briefly into two parts:-- the analytical and the experimental. The procedure of the investigation is outlined in the diagram shown in Fig. 1.

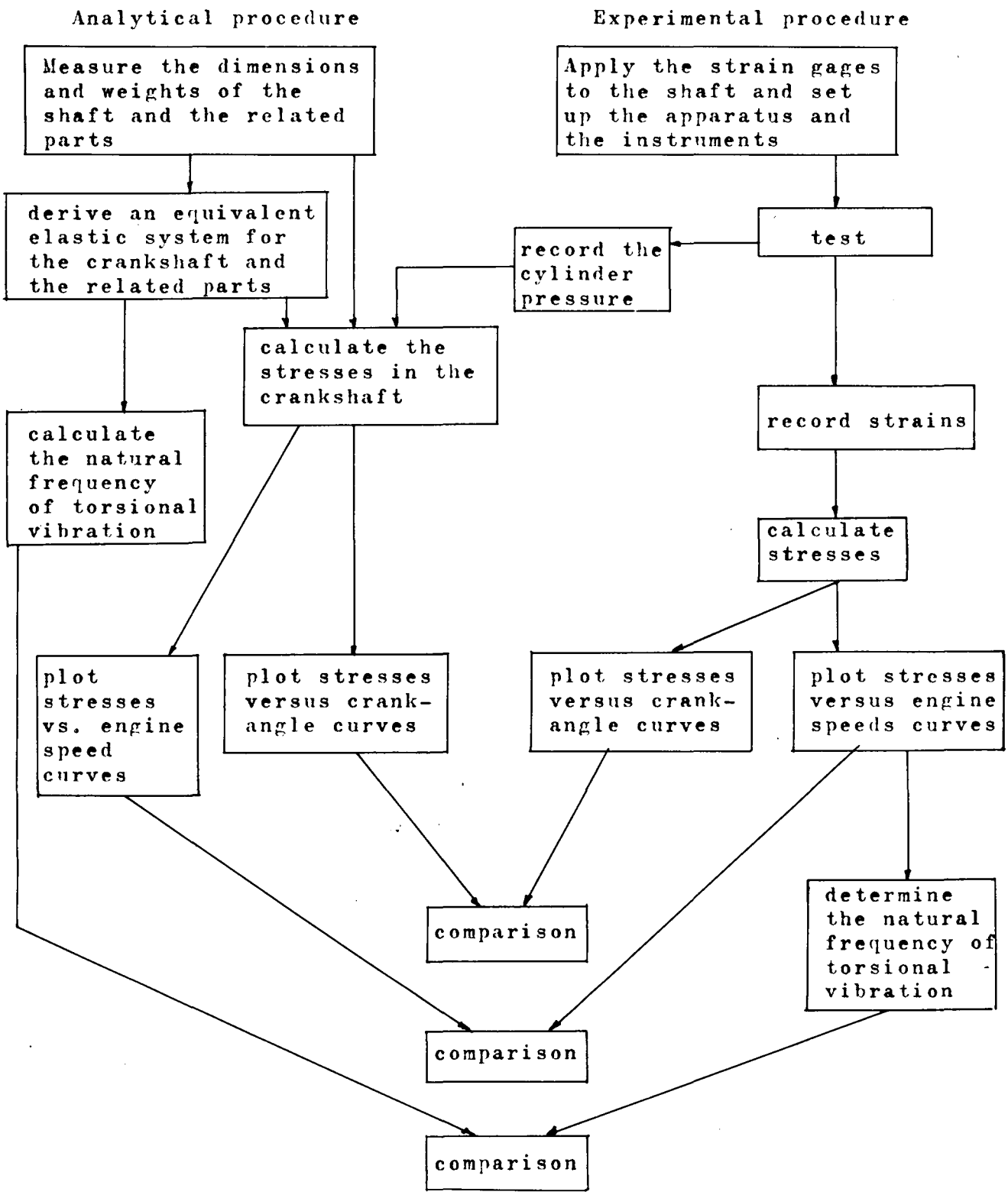

Fig. 1 The outlined procedure of the investigation

1. The Procedure for the Experimental Method

(a) Preliminary to the engine test:

The following points were considered before the test was carried out.

(1) The principle of stress determination --- Actually, the stresses in the crankshaft were not recorded directly, but were calculated from the strains by assuming that the property of the material of the shaft followed Hooke's Law. The strains on the surface of the crankshaft were sensed by strain gages.

The strain gages were made of thin foil or small wire. The thickness of the foil or the diameter of the wire was in the vicinity of one thousandth of an inch. When a strain gage was cemented to a machine part, and the machine part was put under a load, the thin foil of the gage would be stretched or compressed as the machine part was deformed under the load. The geometrical and physical deformations of the foil caused a change in its electrical resistance. The electrical resistance of the gage increased when the gage was stretched and decreased when it was compressed. The change in electrical resistance was due mainly to the change of the cross-sectional area and the change of the total length of the grids of the gage, and the relation between the defor-

mation of the gage and the resistance change in the gage was given by the formula:

$$\Delta R/R = G \cdot \Delta L/L$$

where R = normal gage resistance [ohm]

ΔR = change in resistance [ohm]

L = gage length [inch]

ΔL = change in gage length [inch]

G = a constant, gage factor

If the gage was cemented tightly to the machine part, $\Delta L/L$ was equal to the unit strain on the machine part along the axis of the gage. Thus, when the gage factor was known and the resistance change was detected by electrical instrument, the strain and the stress could be calculated.

Since a single strain gage was only sensitive to strains along its axis, two or more gages were required when the machine part under investigation was subjected to a biaxial load, or a combination of tension, bending, and torsion. After the strains along different axes were recorded the principal stress could be calculated. Also, with various arrangements of the gages and the electrical circuit, it was possible to separate a combined and complex strain pattern into several simple components.

(2) The selection of the engine ---- Any kind of re-

ciprocating internal combustion engine could be used as the apparatus for the test in this investigation. The four-stroke gasoline engine which had a comparatively broad field of application was chosen. Also, since the engine must be taken apart in order to apply the strain gages on the crankshaft, it was preferable to use a small engine to save time and labor in handling it. A 1½ horsepower, single cylinder, air cooled, four-stroke, gasoline engine was selected. The specifications of the engine are given in Appendix A.

(3) The selection of the strain gages --- There were two classes of electrical resistance strain gages available; one made of Constantan or Nichrome V wire, (also in form of foil), and the other made of Iso-elastic wire. The Iso-elastic wire gage had a larger gage factor and was more sensitive to temperature variation, while the Constantan or Nichrome V wire gage was less sensitive to temperature variation and had a lower gage factor.

Since the crankshaft was operating under a dynamic load, the Isoelastic wire gage was more suitable than the Constantan wire gage. However, because the crankshaft was small and the surface on which the strain gages would be located was extremely limited, the size of the gages was also a significant factor. Furthermore, the stresses under investigation were combined stresses,

therefore, rosette form gages were required.

In a review of the manufacturers' catalogs, the writer found that no suitable rosette gage made of Isoelastic wire could be selected to meet the requirements.

The gages finally selected were Constantan foil gages which were made of thin foil by photo-etching techniques. Foil gages have the following improved characteristics over the wire gages:

(a) High longitudinal strain sensitivity

(b) Low transverse strain sensitivity

(c) High fatigue life

(d) Extreme flexibility which means that they can be applied to sharply curved surfaces.

The selected gages were in a 90° rosette configuration. As shown in Fig. 2 in large scale, each rosette gage was composed of two individual gages, and each individual gage had a 120-ohm resistance, a gage length of one-eight of an inch, and a gage factor of 2.1.

(4) The locations of the strain gages on the crankshaft --- The location of the strain gages on the crankshaft is shown in Fig. 3. As shown in the figure, two 90° rosette gages containing the individual gages 1,2, 3, and 4 were applied on the shaft near the flywheel. The axis of each individual gage was orientated at a

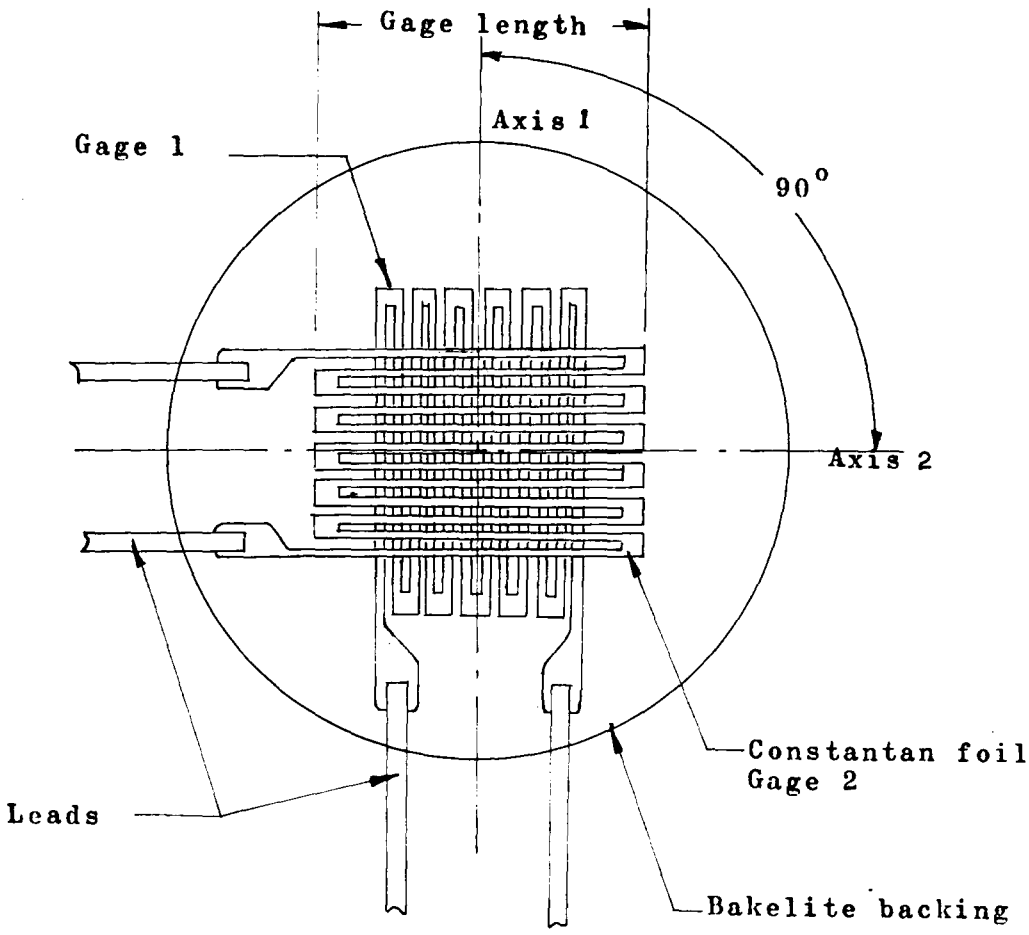

FIG. 2 A schematic drawing of the selected strain gages

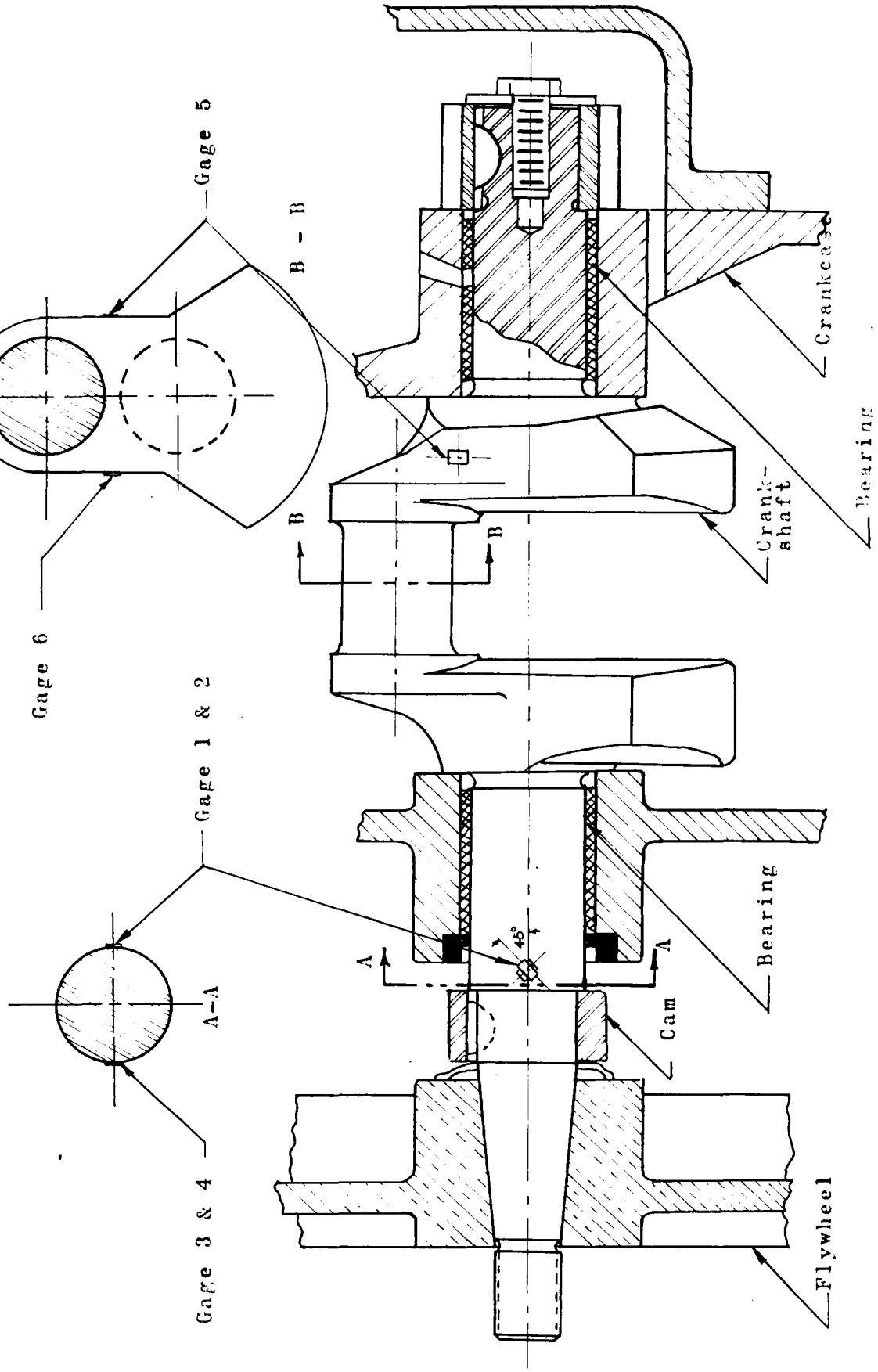

Fig. 3 The locations of the strain gages

45° angle with the axis of the shaft. (The purpose of such an orientation is explained in Appendix C.) These gages were used to investigate the effect of the fly-wheel on the magnitude of the stresses in the crankshaft. As shown in the same figure, two other gages 5 and 6 were applied on the crankweb of the crankshaft. These gages were used to investigate the effect of engine power on the stresses of the crankshaft.

(5) The method for transmitting signals from the strain gages to the recording instruments --- The slip-ring and brush system was selected to maintain an electrical contact between the rotating gages and the stationary instruments recording the signals from the gages. In order to avoid the detrimental effects of the lubricating oil on the contact surfaces between the rings and the brushes, the slip-ring and brush unit was put outside of the crankcase. The slip-rings were attached to the ends of the crankshaft as shown in Fig. 4 and Fig. 5

The slip-ring and brush units shown in Figs. 4 and 5 were miniature slip-ring and brush units manufactured by the Poly-Scientific Corporation, Blacksburg, Va. The rings were made of coin gold and were mounted on a plastic shaft 1/8 inch in diameter. The brushes were made of alloy steel wire of .007 inch in diameter.

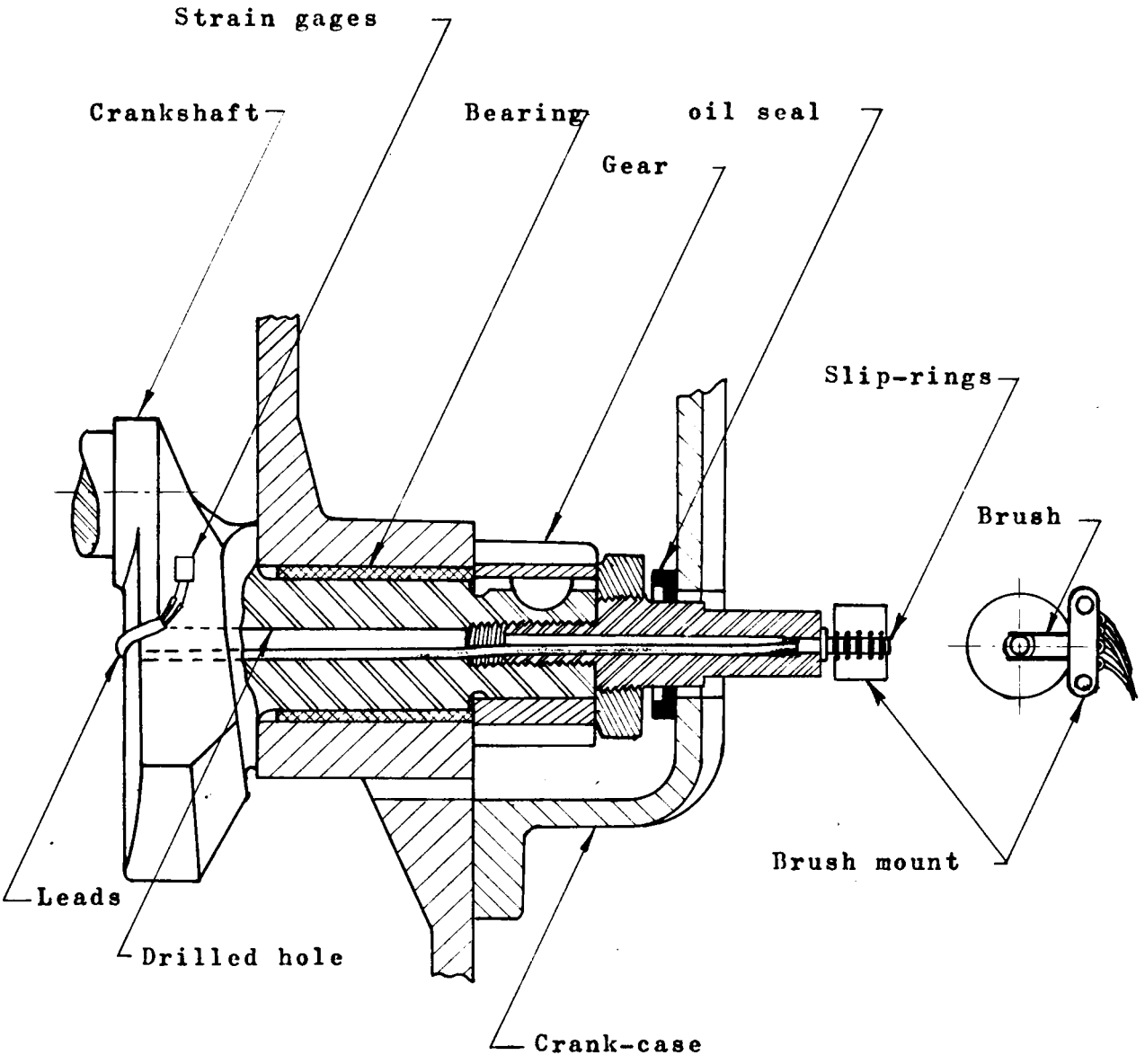

Scale; 1:1

Fig.4 The attachment of the slip-rings to the crankshaft and the passage for the leads.

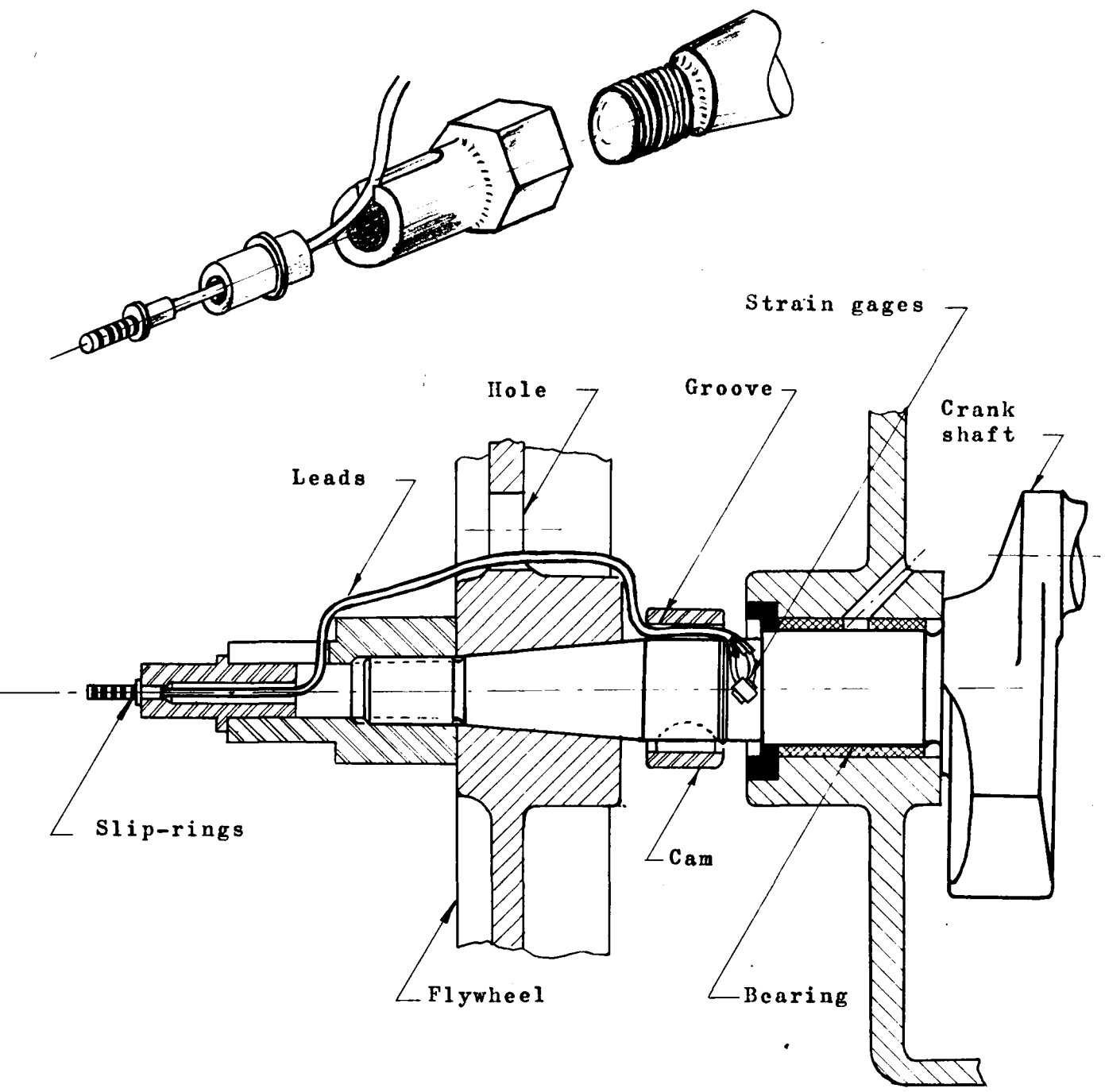

Fig.5 The attachment of the slip-rings to the crankshaft and the passage for the leads. (Some members are omitted from the figure to simplify the illustration)

One end of the brushes was attached to a plastic block while the free end of the cantilever beam rested on the slip-ring. The average noise level (the variation of contact resistance) was about 1 milli-ohm.

(6) The electric circuits used for detecting strain signals --- It is well known that if the resistance of one arm of a balanced Wheatstone- bridge circuit changes, the bridge is unbalanced. The unbalanced voltage across the bridge is indicated by a galvanometer. Thus, the resistance changes in a strain gage can be detected if the gage is connected to a Wheatstone-bridge circuit. With a proper scale the galvanometer can be calibrated to indicate the magnitude of the strain directly.

Also, if two or more gages are connected to a Wheatstone-bridge, the unbalanced voltage indicated by the galvanometer is a resultant of the individual voltages caused by the individual gages. Thus, the magnitude and the property of the resultant voltage depend upon the arrangement of the gages and the magnitude and direction of the resistance change in each individual gage. Three types of arrangement of the strain gages in the Wheatstone-bridge are shown in Figs. 6 and 7. Each arrangement has a different stress to detect.

In Fig. 6(a) gages 1,2,3, and 4 form the arms of the

bridge. This bridge is only senstitve to torsional loads transmitted through the shaft.

In Fig. 6(b) gages 1 and 2 are connected in series to form one arm of the bridge while gages 3 and 4 are also connected in series to form another arm of the bridge. Resistances A and B are some constant resistances used to complete the bridge. In this arrangement the bridge is only sensitive to the bending load imposed on the shaft.

The bridge shown in Fig. 6(c) is arranged for detecting axial loads only. In this circuit gages 1,2,3, and 4 are connected in series and form one arm of the bridge. Resistance A, B, and C are some constant resistances used to complete the bridge.

Since the same gages had to be arranged in three different circuits, as previously mentioned, a switch system was required to facilitate the shift from one circuit to another. The switch system is shown in Fig. 11.

(7) The recording instruments --- In addition to the basic galvanometer, various electronic instruments can be used to indicate and register the unbalanced voltage across a Wheatstone-bridge circuit. An oscilloscope was used for this purpose in this investigation.

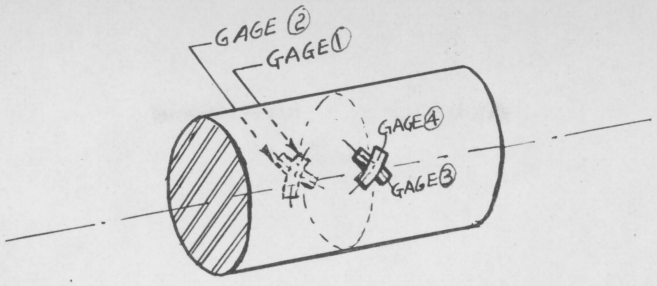

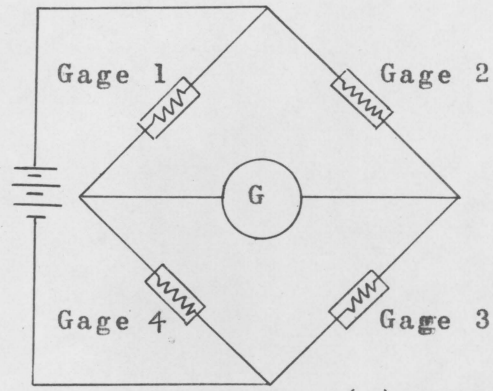

(a) The Wheatstone-bridge circuit used to detect torsional stresses

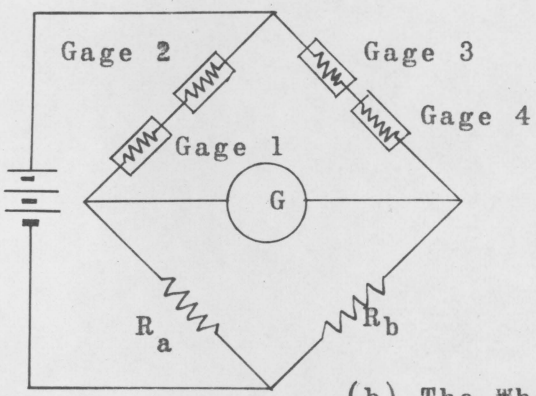

(b) The Wheatstone-bridge circuit used to detect bending stresses

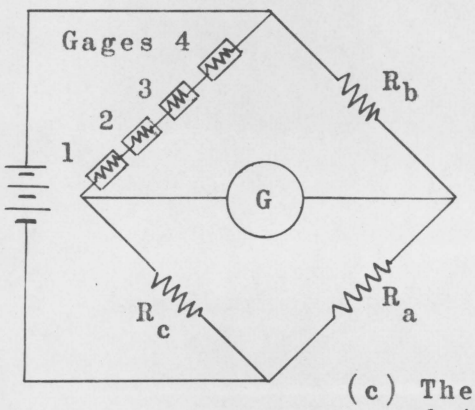

(c) The Wheatstone-bridge circuit used to detect stresses due to axial thrust

Fig. 6 The circuit arrangements of the strain gages

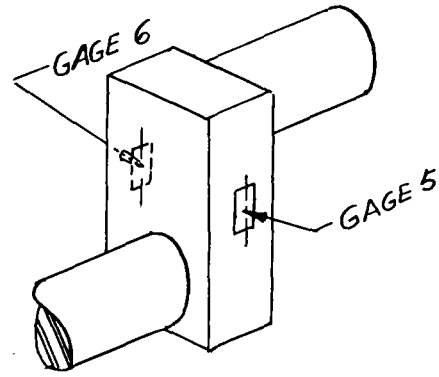

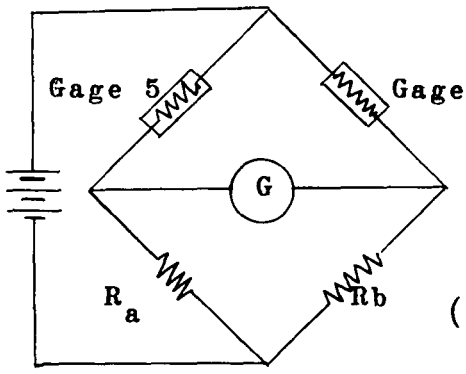

(a) The Wheatstone-bridge circuit used to detect bending stresses

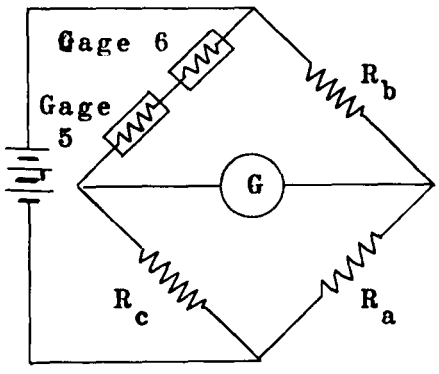

(b) The Wheatstone-bridge circuit used to detect axial stresses

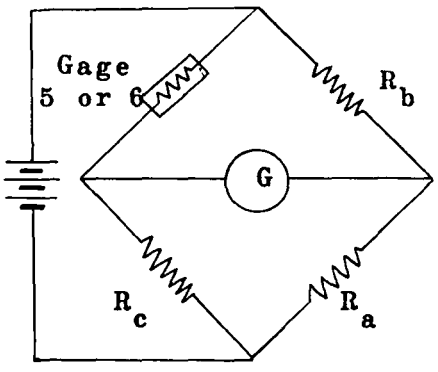

(c) The Wheatstone-bridge circuit used to detect total stresses along the axis of the related strain gage.

Fig. 7 The circuit arrangements of the strain gages

Since the output voltage from the Wheatstone-bridge was not high enough to operate the oscilloscope, the signals from the bridge had to be amplified before they entered the oscilloscope. A bridge-amplifier which was particularly designed for the application of strain gages was used. The amplifier contained an amplifying circuit, a bridge circuit, a calibrating circuit, a measuring circuit, some adjustible resistance, and batteries.

When the amplified unbalanced voltage entered the oscilloscope, it caused a vertical deflection of the cathode-ray, and the ray displaced a vertical trace on the fluorescent screen of the cathode-ray tube. Since the height of the deflection is linearly proportional to the unbalanced voltage, the deflection of the ray is also linearly proportional to the strain. With a proper scale the vertical displacement of the cathode-ray was calibrated to indicate the strain directly.

In addition to the vertical displacement, the cathode-ray also displaced horizontally. The horizontal sweep was produced by an oscillator circuit built into the oscilloscope. This circuit produced a saw-tooth form oscillation voltage on the horizontal deflection plates of the cathode-ray tube and caused the spot on the fluorescent screen to start at the left-hand side of the field

moving from left to right at a constant velocity and then to return almost instantaneously to the left to repeat the travel. Therefore, the horizontal sweep of the cathode-ray provided a time abscissa with which to correlate the vertically displaced strain signal. By synchronizing the engine speed with the horizontal sweep time of the cathode-ray, a strain versus crank angle curve could be recorded directly.

In order to initiate the horizontal sweep of the spot on the oscilloscope at the same precise point in the engine cycle, an external triggering device was used in addition to the automatic oscillator circuit as previously mentioned. The triggering device was composed of a trigger-pin mounted on the camshaft of the engine and a stationary inductive coil. A voltage pulse was generated when the magnetic field surrounding the inductive coil was disturbed by the trigger-pin passing by. This voltage pulse was put in to the oscilloscope to start the horizontal sweep of the cathode-ray. The trigger-pin and the inductive coil were mounted at such a relative position that a sharp voltage pulse was generated when the piston of the engine was at the top-dead-center position before the power stroke. Since the trigger-pin was mounted on the camshaft, a voltage pulse was generated at each

complete engine cycle. With this triggering device, the trace of the cathode-ray always started at the left side of the fluorescent screen as soon as the power stroke of the engine began, then it displaced the strain signal vertically while it was sweeping at a constant velocity to the right.

The trace which was displaced by the cathode-ray on the oscilloscope was recorded by a specially adapted polaroid-land camera.

A pressure indicator was used to indicate the gas pressures in the cylinder of the engine. The indicator contained a sensing tube attached to a metal diaphragm. The sensing tube was composed of a thin wall tube, and two 1000-ohm strain gages attached to the outside surface of the metal tube. When the metal diaphragm was deformed under the cylinder pressure, it compressed the sensing tube and changed the resistance of the attached strain gages. Signals corresponding to the cylinder pressure were recorded by the same electric circuits and instruments as previously described.

(8) The system for engine control --- Since the stresses in the crankshaft of the engine were investigated at various conditions, a control system was required to adjust the engine load and engine speed.

The control system consisted of a direct current generator, a resistance rack, a rheostat, and a rectifier. When the generator was driven by the engine, it converted the power delivered by the engine into electrical energy, then the electrical energy was converted into heat through the resistance rack and the rheostat. Thus ,by changing the total resistance across the resistance rack and the rheostat, the engine load and the engine speed could be adjusted. Also, when the generator was connected to an electric power source, it became a motor and was used to drive the engine. In this arrangement the resistance rack and the rheostat were used to adjust the speed of the generator. The rectifier was used to supply direct current.

(b) The arrangement of the apparatus and the instruments:

(1) The application of the strain gages to the surface of the crankshaft --- As shown in Fig.2 the thin foil of the strain gage was cast in a backing material Bakelite. This backing material and the gage itself were attached to the surface of the shaft by cement. A cement which has the same properties as the backing material (and is also named Bakelite Cement) was used. In order to ensure a proper attachment, it

was necessary to clamp the gages to the surface of the shaft during the drying period. And also, heat treatment was required to cure the cement to obtain a proper performance of the gages.

The clamping devices are shown in Fig.9. Each clamp was composed of three wooden blocks guided by two steel rods, a spring, and a C-clamp. The wooden blocks were cut to fit the curvatures of the circular shaft and the crankweb to provide a uniformly distributed clamping pressure on the gages. The spring was used to maintain a constant clamping pressure on the gages, and the C-clamp was used to apply force.

The surface on which the gages were to be installed was first roughened by a medium grade emery paper, and then it was cleaned with acetone. After the surface was cleaned and dried, a thin coat of Baklite cement was applied to the surface. The gages which were also cleaned with acetone were then placed over the cement. A piece of cellophane and a felt pad were placed over each gage, and finally the clamping devices were applied.

The heat treatment was carried out in an oven. The baking cycle was one hour at 175°F followed by two hours at 250°F and two hours at 330°F.

(2) The arrangement of the circuits for data re-

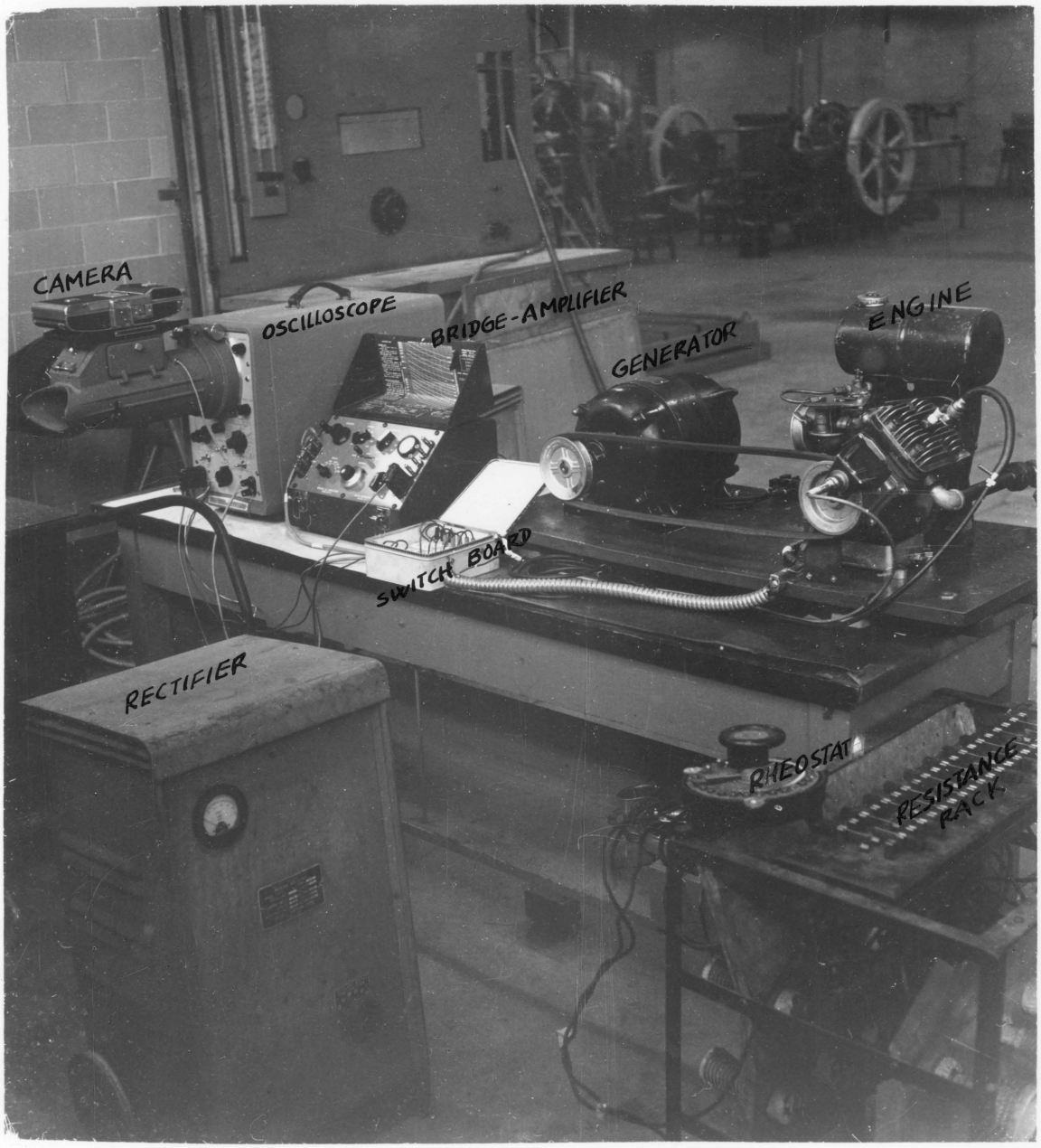

FIG. 8 The apparatus and the instruments

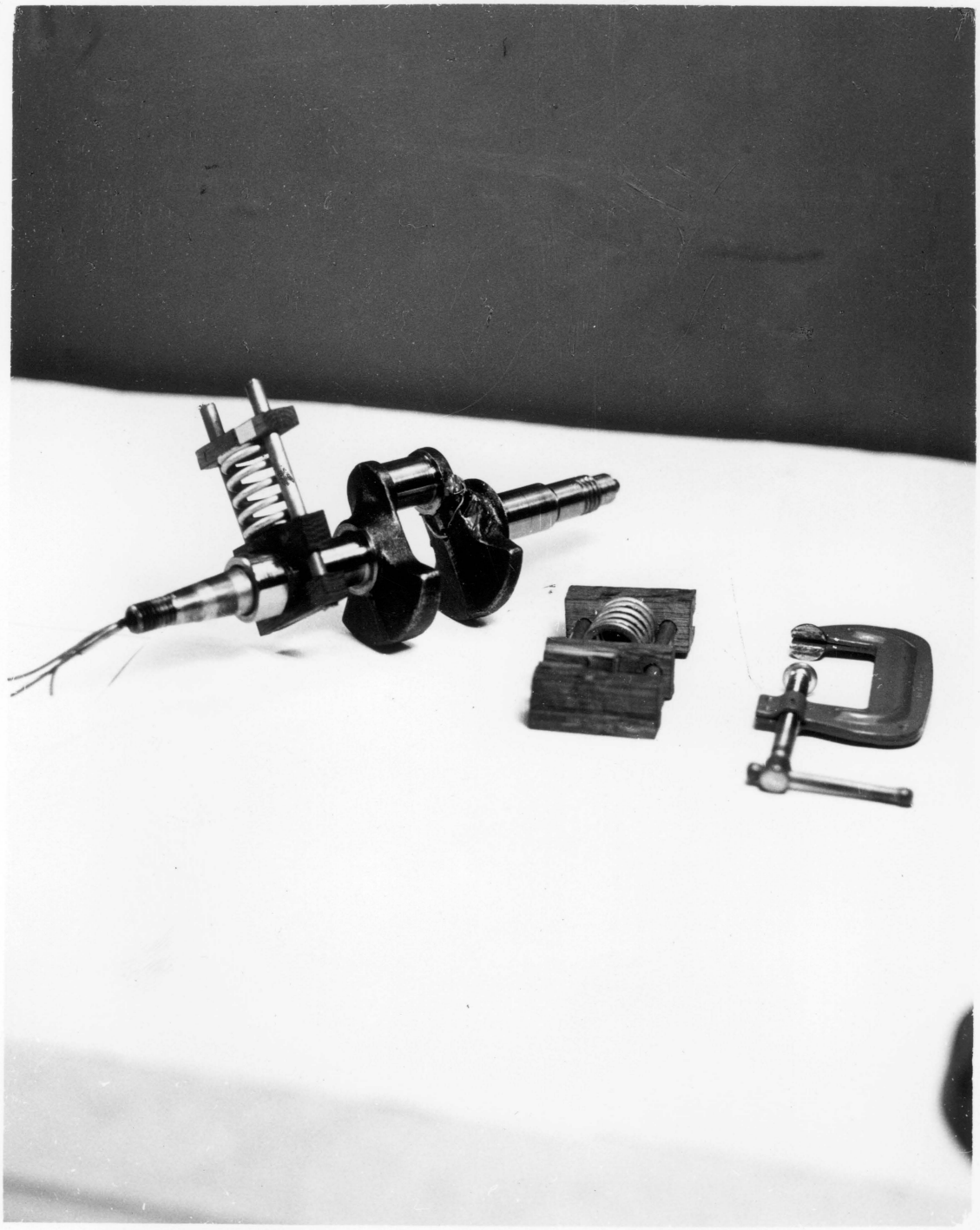

FIG. 9 The application of the strain gages on the shaft

cording --- The circuits which were used for recording data are shown in Fig.10. As shown in the figure, the leads from the strain gages and the leads from the pressure indicator were first connected to a switch board, and then they were connected to the leads from the instruments to complete the proper circuit for the test. The switch board and the switches are shown in Fig.11. They were designed to provide a quick operation.

(3) The circuits for engine load and engine speed control --- The connections between the generator, the resistance rack, the rheostat, the rectifier, and the control switches are shown in Fig.12. As shown in the figure, when the switches are turned to the positions designated by (M), the circuit is used for motor speed control. When the switches are pushed to the positions designated by (L), the circuit is used for engine load control.

(4) The alignment of the triggering device --- To install the triggering device a hole was tapped through the rim of the camshaft pulley. The triggering pin which was made from the body of a machine screw was screwed half way into the tapped hole. An angle plate was used to support the inductive coil from the engine frame. Since the pin and the center of the inductive coil must

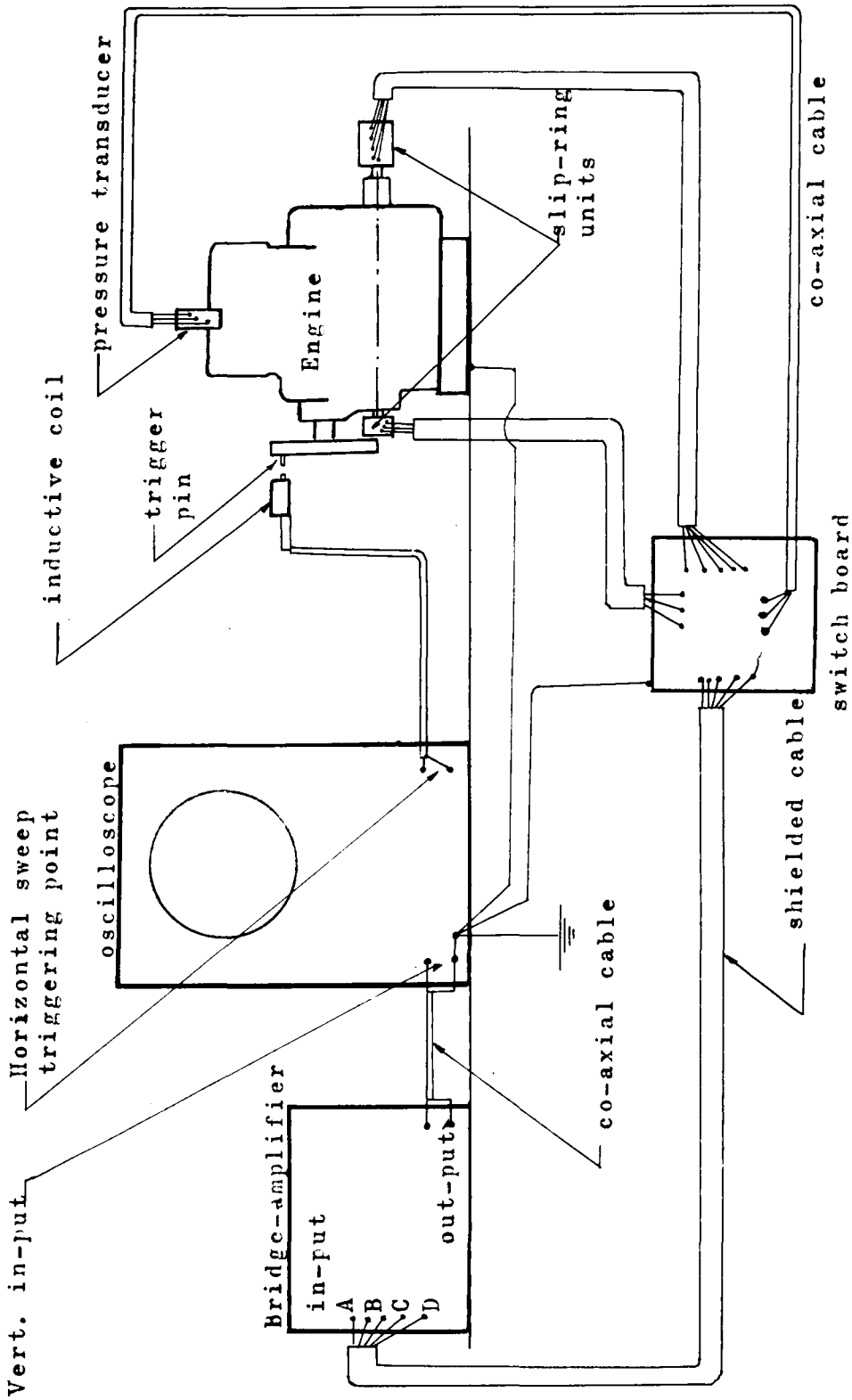

Fig. 10 The connections of the electric circuit for data recording

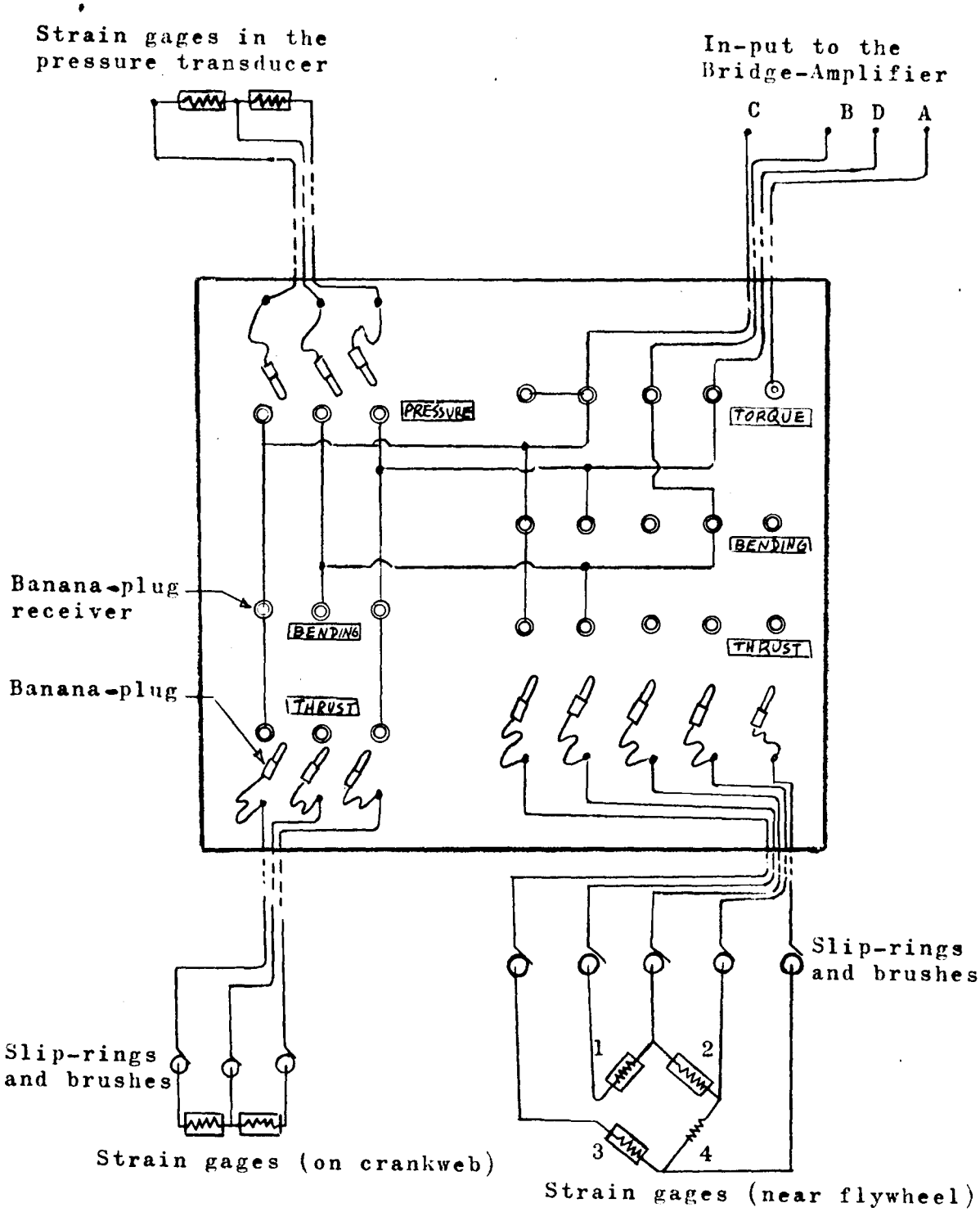

Fig. 11 The switch board

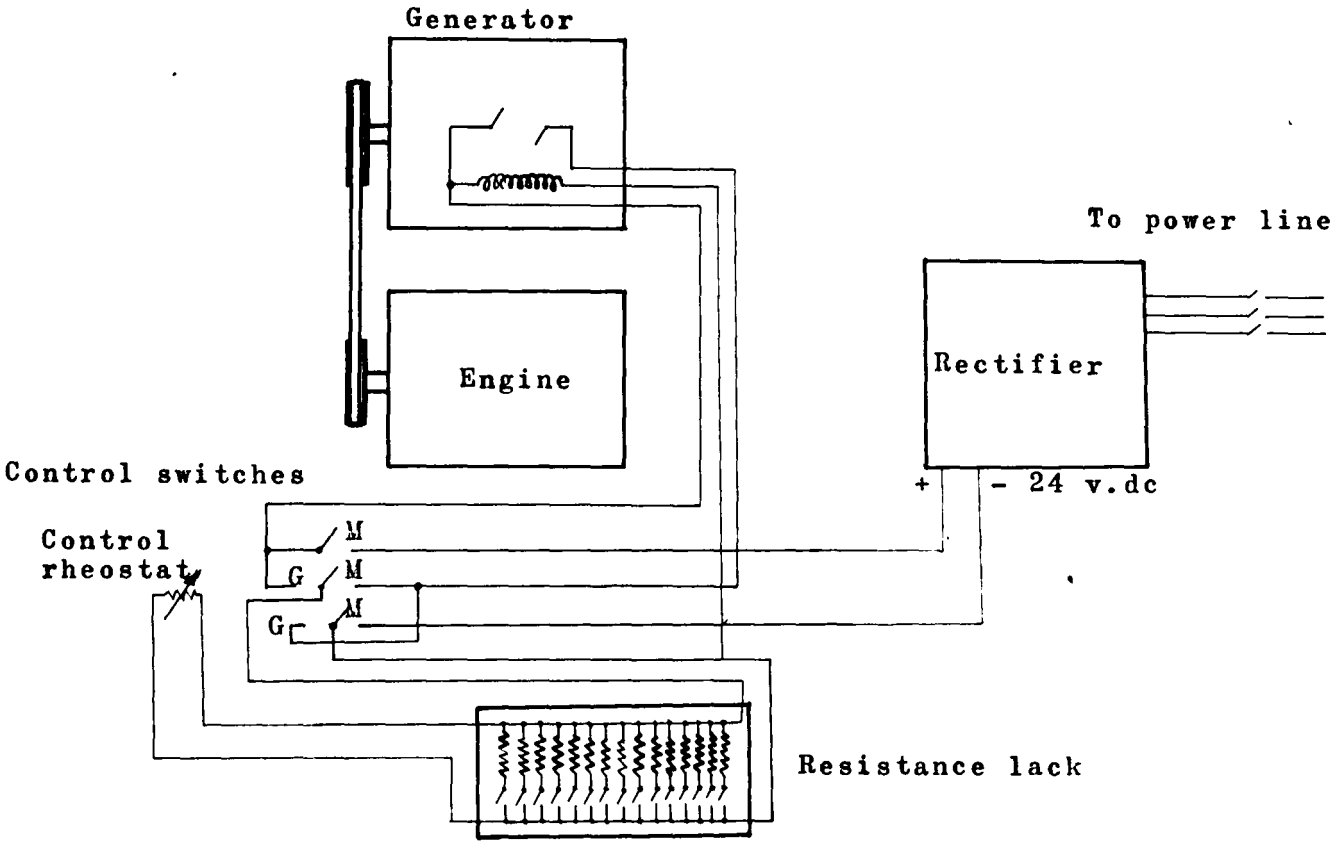

-/- -- Switch

(M) -- Switch position for motor control

(G) -- Switch position for engine control

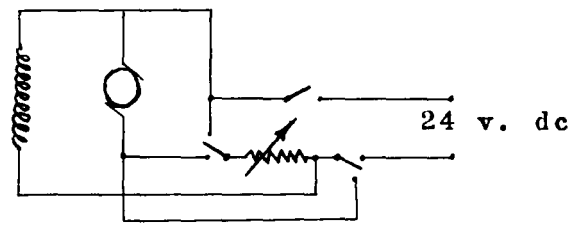

The outlined circuit

Fig. 12 The connection of the electric circuit for engine and motor control.

be aligned when the piston of the engine is at the top-dead-center position, the corresponding position of the camshaft had to be determined first. This was done by using a dial indicator. With the cylinder-head removed the dial indicator was mounted on the cylinder block so that the piston of the engine was in contact with the contact point of the indicator. By turning the crankshaft, the piston was brought to the position corresponding to the end of the compression stroke. Then, the crankshaft was turned slowly forward and backward and was stopped at the position at which the reading on the dial indicator was maximum. With the crankshaft held at this position, the inductive coil of the triggering device was adjusted to align with the pin.

(c) The calibration of the instruments:

The following miscellaneous tests and calibrations were made on the apparatus and the instruments:

(1) The calibration of the pressure transducer --- As previously mentioned, the pressure in the cylinder of the engine was sensed by a pressure transducer and the magnitude of the pressure was indicated as the height of deflection of the pressure signal shown on the os-

cilloscope. The relation between the height of deflection of the pressure signal and the pressure acting on the pressure transducer was calibrated by the use of a dead weight tester.

The height of deflection of the pressure signal shown on the oscilloscope was recorded for each known weight applied on the dead weight tester. The corresponding pressure was calculated for each of the weights applied. Then, the calculated pressures were plotted in a curve against the recorded height of deflection. With this curve the cylinder pressure could be read directly from the oscilloscope.

(2) The calibration of the engine speed against the setting of the control devices --- In order to facilitate the control of the engine, the engine speed at each setting of the throttling valve and the rheostat was determined. Then, a dial indicating the engine speed was made and mounted on the rheostat so that a quick adjustment of the engine speed could be made.

(3) The test of the characteristic of the triggering device --- This was done by charging the voltage pulse generated by the inductive coil of the triggering device into the oscilloscope. The pattern of the voltage

pulse was observed and recorded.

(4) The setting of the recording camera -- In order to obtain a clear and significant picture of the signals shown on the oscilloscope, various combinations of the setting of the iris diaphragm, the exposure time, and the brightness of the signal were tried. The best combination was obtained with the iris diaphragm set at f = 4.5. The scale light on the oscilloscope was set at about one-third of its maximum brightness and was left on for each super-imposed exposures. The setting of the horizontal sweep time of the cathode-ray and the setting of the film exposure time were given by the following formulas.

$$\text{Sweep time} = \frac{1}{\frac{N}{2\times60} \times W} = \frac{8}{N} \quad [\text{sec/cm}]$$

$$\text{exposure time} = \frac{1}{\frac{N}{2\times60}} = \frac{120}{N} \quad [\text{sec/cm}]$$

where N -- engine speed rpm

W -- width of the screen of the oscilloscope = 15 cm

(d) The technique in taking data:

As previously mentioned the strain signal as shown

on the screen of the oscilloscope is in form of a curve, and it was recorded by taking pictures of the screen with a specially adapted polaroid-land camera. The procedure is briefly described as follows:

After the apparatus, the circuits, and the instruments were carefully checked, the oscilloscope and the amplifier were turned on for a warm up period; then, the rectifier was switched on, and the switches in the engine control circuit were pushed to the "G" positions (see Fig.12) to run the generator as a motor. Driven by the generator, the engine was started after a few revolutions. As soon as the engine was started, the switches in the engine control circuit were pulled back over the "Off" position to the "M" position to put the generator and the resistance rack into a power absorbing circuit. By controlling the rheostat and the throttling valve, the engine was brought to a steady speed. The engine speed was indicated and recorded with a hand tachometer. The engine was kept running for a warm-up period while the leads from the pressure transducer were switched to the recording instruments. The signal corresponding to the cylinder pressure was then observed on the screen of the oscilloscope. With adjustments made on the "Vertical Sensitivity" control and the "Vertical Position" control, the signal was

brought to the center of the screen and was enlarged to the hightest rate of amplification. Then, the engine was stopped. After the engine was stopped, the signal shown on the oscilloscope was a horizontal straight line which corresponded to the zero strain axis. This line was recorded with the camera immediately. Then, the engine was started again and was kept running at the original speed. The external triggering unit was switched on to take over the function of the automatic internal triggering unit, and a steady pressure signal curve was then observed on the oscilloscope. With the adjustment made on the "Horizontal sweep time" control, the pressure signal was adjusted so that only a complete cycle of the cylinder pressure was shown on the screen. Then, with the camera still at its original position the pressure signal curve was recorded. This second exposure of the film was super-imposed on the first one. The leads from the pressure transducer were disconnected from the amplifier and the "Measure" switch on the Bridge-Amplifier was switched from the'Measure' position to the "Calibration " position. A chopped calibration signal was then seen on the screen of the oscilloscope. Once again,the calibrating signal was recorded and superimposed on the first two exposures. The camera was

then slipped from its outer position to the inner position to bring the second film into position for the next recording.

With the engine still running at the original speed the "Measure" switch was pushed back to the "Measure" position, and the leads from the strain gages 1,2,3, and 4 were connected to the amplifier through the "Torsion circuit", (see Fig.11). The signal which was observed on the oscilloscope was then the torsional strain in the crankshaft. The signal was adjusted to the best position on the screen and was recorded by the camera. The engine was stopped. The internal triggering unit was switched on and the zero-strain axis was recorded. Once again, the calibrating signal was brought in and recorded. The zero-strain axis and the calibrating signal were super-imposed on the strain signal.

The first set of film which included two pictures each containing three super-imposed exposures was pulled from the recording position to the developing position. The time required for development was 80 seconds. Then, the developed pictures were taken out from the top of the camera.

The engine was started again and was kept running at the same load and engine speed as the previous

run. Then with the same procedure as previously described, the leads from the gages 1,2,3, and 4 were rearranged and were connected to the amplifier through the "Bending" circuit. The signal which indicated the bending stresses on the surface of the crankshaft was then observed on the oscilloscope. After the signal was adjusted so as to have the best position and the best stage of amplification, it was recorded with the camera. Once again the calibrating signal was brought in and recorded. The engine was stopped and the zero-axis was recorded.

The above procedure was repeated until all the strain signals from different gages and from different circuits were recorded. Then, the whole procedure was repeated for different combinations of engine speeds and engine loads.

A record of the successive torsional strain signals in a range of engine speed was also made. First, the engine was driven by the generator at the lowest speed, the camera was pulled up to its outer extreme position on the sliding mechanism, and a record of the strain signal was made, Then, the engine was allowed to run at a slightly higher speed, the camera was moved inward about one tenth of the total distance between the outer and inner extreme positions, and the strain signal was

recorded on the same film. Once again, the engine speed was increased slightly while the camera was moved further inward to record the signal. The procedure was repeated until the camera reached the inner extreme position. The film was then developed.

2. Difficulties Encountered During the Investigation and How They Were Solved.

It has been mentioned by many users that small strain gages were difficult to apply, and that certain techniques were required in applying small strain gages. Therefore two low cost strain gages were used to make a preliminary test before the selected strain gages were applied. The preliminary test was helpful; it exposed certain points which had been over-looked before the test.

The main difficulty was that a considerable error of the strain signal was caused by electrical disturbance. The electrical disturbance included all the electrical interference from other equipment operating near the test apparatus and the electrical interference from the internal source--the apparatus, instruments, and circuits. The internal source of disturbance was mainly the contact resistances between the slip-rings and the brushes of the slip-ring unit which was used to maintain an electrical contact be-

tween the strain gages and the recording instruments. The disturbance from the external source was later reduced to a satisfactory level by proper grounding and shielding of the apparatus and the instruments. However, the electrical disturbances from the internal source posed a problem.

As claimed by the manufacturer, the previously selected slip-ring unit had an average noise level of 1 milli-ohm. The unit was considered to be accurate enough since the strain gages had a change of resistance of 0.07 ohm which corresponding to a stress of 2000 pounds per square inch. However, because the engine vibrated severely during the test, a high brush pressure was required and the slip-rings were worn rapidly. The noise level was increased to 13 milli-ohms after a few hours operation. The test was thus discontinued until a satisfactory slip-ring unit was developed.

The characteristics of various types of slip-ring and brush units employing the solid to solid contact method have been reported by several investigators, (see Review of Literature p.13), and the materials and required contact pressure for a satisfactory slip-ring unit were suggested. However, it has also been mentioned that the noise (the electrical interference) could not be eliminated entirely because the noise was caused by the local oxidation and the wear of the contact surfaces between the rings and the

brushes. It seemed to the writer that a liquid-to-solid contact method should be used in order to reduce further the noise of the slip-ring unit.

In the first attempt of developing a liquid-to-solid slip-ring, mercury was used as the intermediate medium filling the space between a rotating ring and a stationary iron plate. A test on this unit showed that although noise still existed, the level of the noise was observed to be reduced in comparison to the noise of a solid-to-solid slip-ring unit. A comparison of the noise generated by a solid-to-solid slip-ring unit to the noise generated by a liquid-to-solid unit is shown in Fig. 13. From this figure it is obvious that the liquid-to-solid slip-ring would cause less error in the strain signal than the solid-to-solid one.

Since no previous investigation had been made on the liquid-to-solid type slip-ring unit, a series of improvement had to be make before a satisfactory one was obtained.

Mercury was still used as the liquid medium in the slip-ring unit because no chemical reaction occurs when two metal plates were brought together. However, because of the high surface tension of mercury it did not wet the metal surface well. As shown in Fig. 14(a) dust was attached on the surface of the metal plate and thus provided a bad electrical contact. This difficult was solved by the method described below.

(a) Noise of the liquid to solid contact slip-ring unit

(b) Noise of the solid to solid contact slip-ring unit

(c) Noise of the liquid to solid contact slip-ring unit at high stage of amplifiaction

(d) Noise of the solid to solid contact slip-ring unit at high stage of amplification

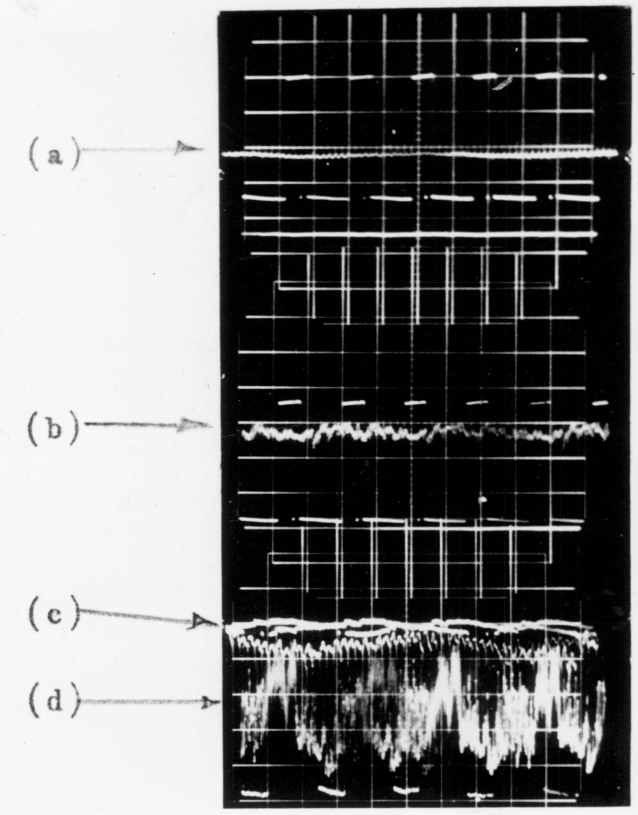

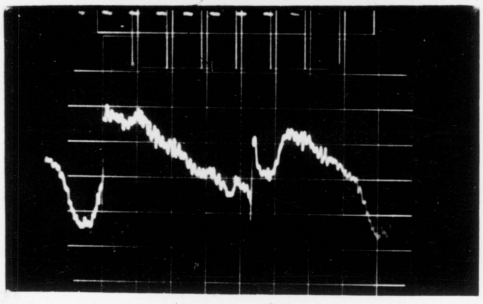

(e)

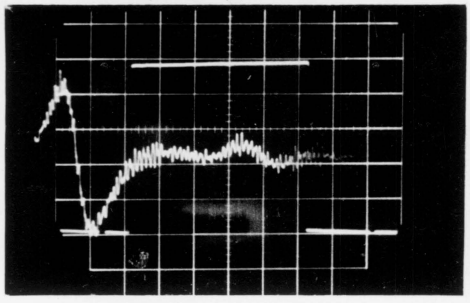

(g)

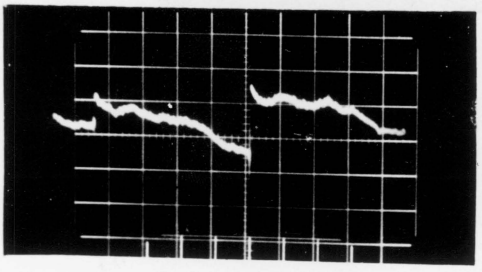

(f)

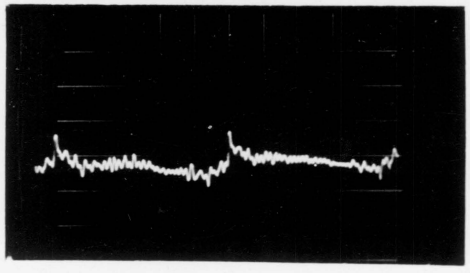

(h)

Fig. 13 The characteristics of the noise of the slip-ring units and the ignition unit of the engine.

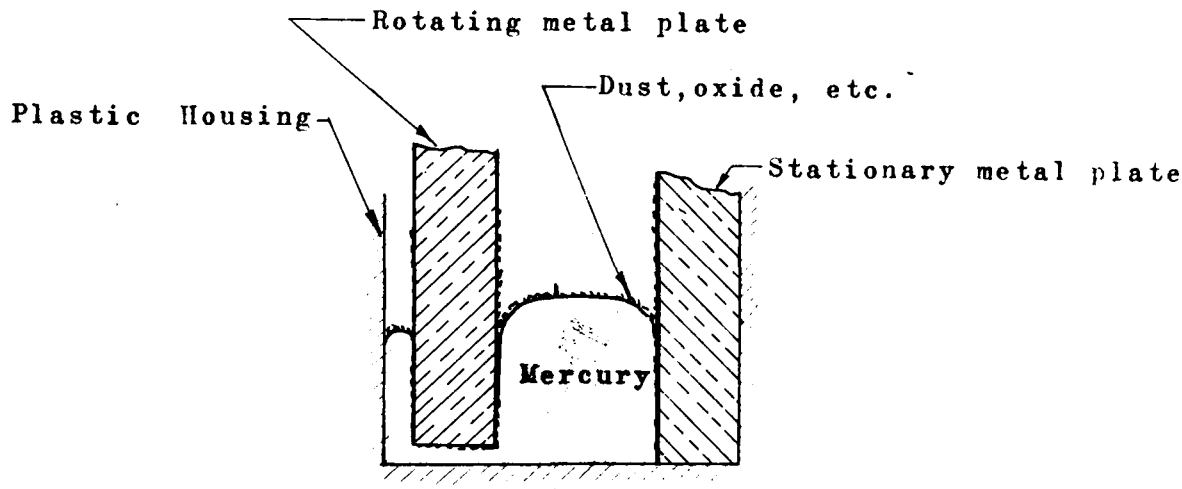

(a)

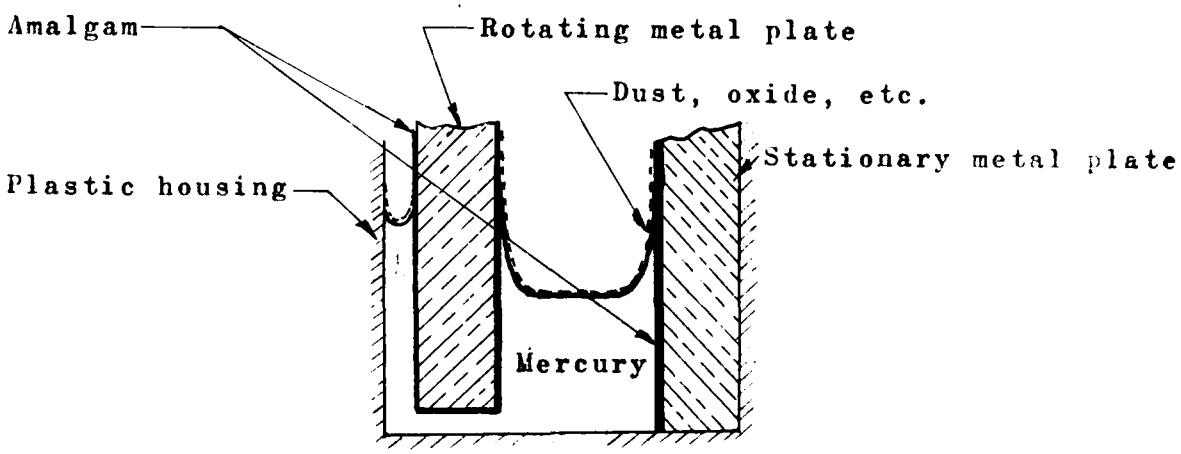

(b)

Fig.14 The effect of amalgam on the contact surfaces between the metal plate and the mercury.

Since most of the metals dissolve in mercury to form a metallic solution, amalgam, a good electrical junction between a metal plate and mercury can be accomplished by forming a layer of amalgam between them. The formation of amalgam depended upon the solubility of the metal in the mercury. Some light metals such as sodium dissolve in the mercury easily while the heavier metals only dissolve slightly. The iron plates which were used to build the slip-ring unit in the first trial were replaced by copper plates because of the small solubility of iron in mercury. The formation of a thin layer of copper-mercury alloy on the surface of the copper plate was achieved by dipping the copper plate into a mercuric nitrate solution (about 5-10% by weight). Under chemical reaction, the mercury molecules in the solution were replaced by the copper molecules and were deposited on the copper plate. A layer of amalgam was formed when some copper molecules mixed with the deposited mercury.

The result of the surface treatment is illustrated in Fig. 14(b). It is obvious that a perfect contact was provided.

The construction of the slip-ring unit is shown in Fig. 15. Because the size of the slip-ring unit was limited by the available space, a complete seal between the rotating shaft and each of the compartments containing the mercury could not be provided without difficulties. After several

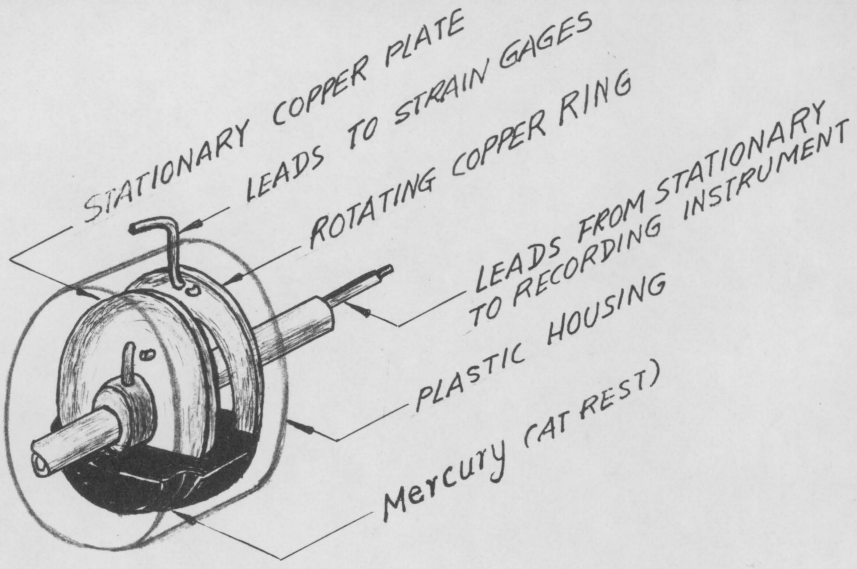

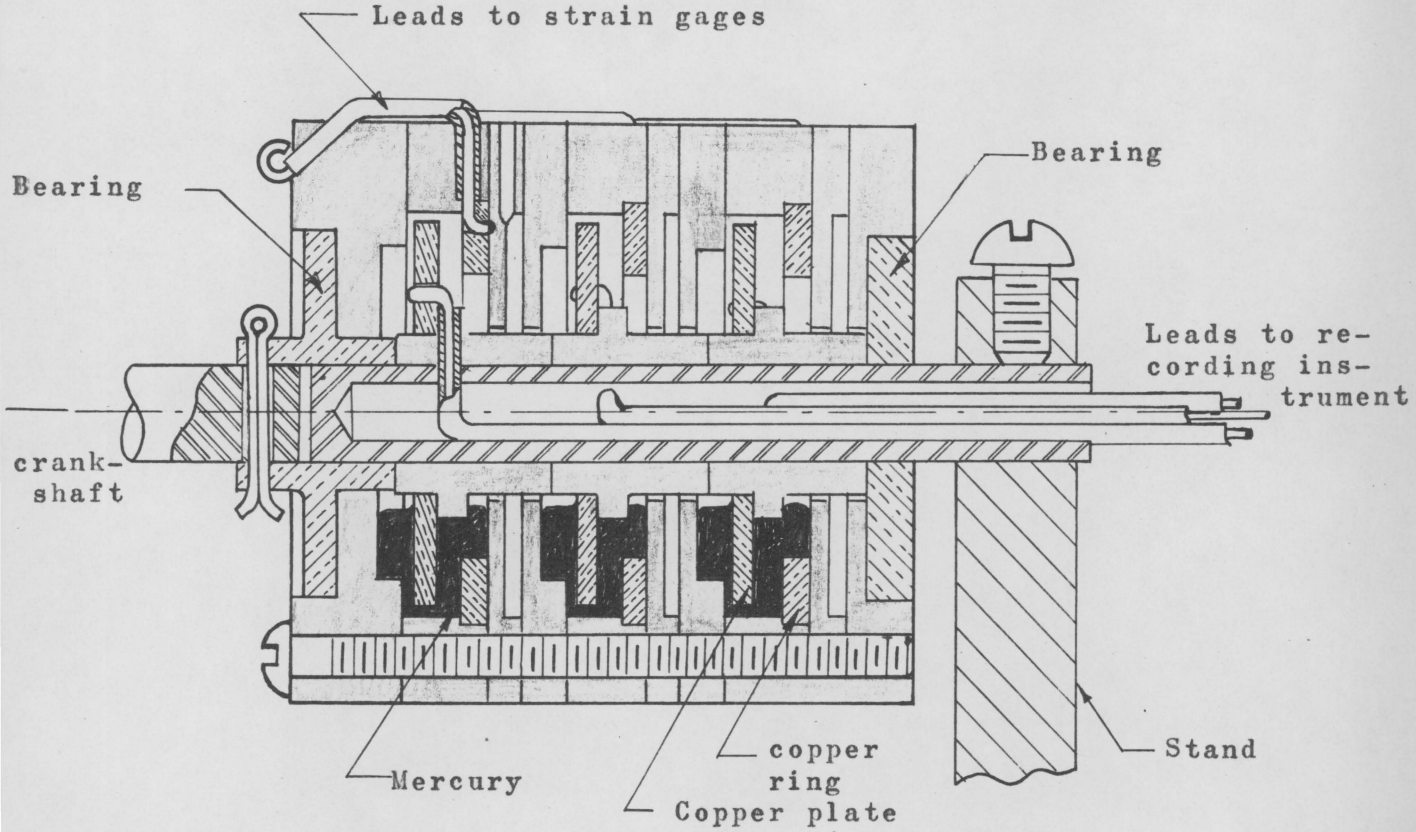

Fig.15 The Construction of the 'Solid to Liquid' slip-ring unit

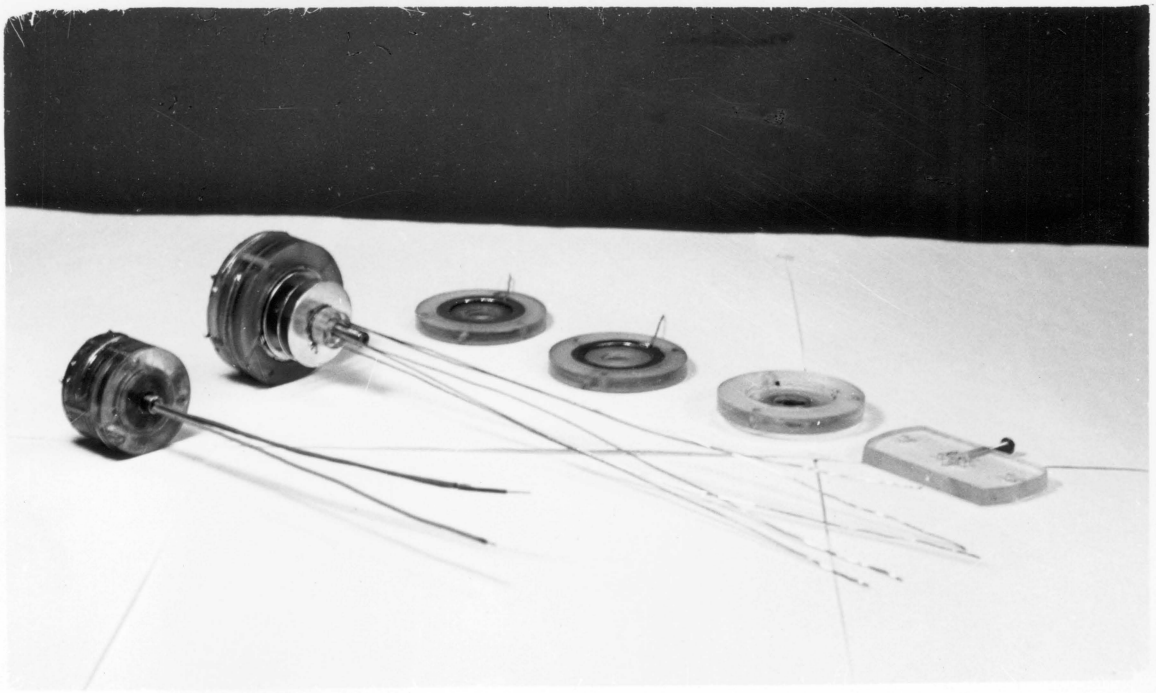

FIG. 16 The construction of the liquid-to-solid slip-ring units

FIG. 17 The mounting of the slip-ring units to the shaft

different designs of the housing had been tried, the construction shown in Fig. 15 was finally used. As shown in the figure each of the compartments of the housing is approximately half filled with mercury. The housing is connected to the shaft of the engine by a universal joint. As the engine runs, the mercury is thrown against the inner surface of the circular compartments of the housing. A mercury ring is thus formed in each compartment while the stationary copper plates work as the brushes.

Some noise was still observed after a series of improvements had been made on the liquid-to-solid slip-ring unit. However, satisfactory results were obtained by the application of this unit to the final test. The noise generated by this unit had a pattern similar to a high frequency wave. As shown in Fig. 13(g) the effect of the noise on the strain signal is similar to the effect of the carrier wave on a sound wave in a telephone line. The actual signal curve is therefore represented by the neutral axis of the noise wave. The actual strain curve was obtained by drawing the neutral axis of the noise wave, and the noise of the slip-ring was thus entirely eliminated. (The noise generated by a solid-to-solid slip-ring unit could not be eliminated in this way because the noise pattern was irregular).

Several attempts were made to reduce the electrical

disturbance caused by the ignition unit of the engine. The disturbance was observed when the engine ran under its own power. (The ignition unit was removed when the engine was driven by the generator). The first record of the disturbance is shown in Fig. 13(e). As shown in the figure, a sharp jump of the strain signal occurred at the point where a spark was set off at the spark-plug. The disturbance was studied by using four dummy strain gages placed near the active gages. Since the dummy gages were not sensitive to the strain, the signal recorded from these gages showed the disturbance only. A record of the disturbance is shown in Fig. 13(f).

The disturbance caused by the ignition unit was reduced slightly after shielding and grounding the entire ignition unit. However, the strength of the disturbance was still high and had a pattern as shown in Fig. 13(h). Since the disturbance was observed to have a steady pattern, the true strain signals were obtained by substracting the noise signals from the recorded strain signals.

3. The Analytical Procedure

(a) The Assumptions:

In order to simplify the calculations the following assumptions were made:

(1) The frictional forces were neglected.

(2) The force acting on the main bearings of the engine were assumed to be concentrated and acting at the center of the bearing.

(3) The inertia masses of the connecting rod was equivalent to two concentrated masses, one located near the piston, and the other at the center of the crank pin.

(4) At a given load and engine speed, the torque transmitted to the generator was nearly a constant.

(b) The Sources of the forces acting on the crankshaft:

The stresses in the crankshaft are induced by forces from two sources. These forces are:

(1) The external forces acting on the crankshaft --- These include the forces from the combustion chamber transmitted through the connecting rod to the shaft, the inertia forces of the piston, the inertia force of the connecting rod, the bearing pressure, and the reaction torque from the generator.

(2) The inertia forces of the crankshaft itself --- These include the centrigugal forces and the effect of vibration.

The calculations were started from the power source -- The gas pressure in the combustion chamber. The cylinder pressure was obtained from a pressure transducer as previously mentioned, and the analytical results were obtained from the same engine condition at which the experimental results were obtained.

(c) The Forces:

As shown in Fig. 18 the cylinder pressure, p_p, at a crank angle θ is obtained from the recorded pressure diagram. Let F_p be the total force acting on the piston, and F_r be the total inertia force of the piston and the small end of the connecting rod. F_p and F_r are obtained from the following formulas:

$F_p = A \times p_p$ where A = area of the piston in.

N = engine speed rpm.

$F_r = 9.06 \times 10^{-6} \times N^2 (\cos \theta + 0.28 \cos 2\theta)$

(see Appendix B)

F_r is added to F_p to obtain F_s, and F_b is a force of F_s acting along the axis of the connecting rod. F_c is the centrifugal force of the big end of the connecting rod and is obtained from the following

formula:

$F_c = 3.48 \times 10^{-6} \times N^2$ (see Appendix B)

F_R is the resultant force of F_b and F_c and is the total force acting on the crank-pin of the connecting rod. F_t and F_a are the tangential and the axial components of F_R. R_x, R_y, G_x, and G_y are the bearing reactions, and T_1 and T_2 are the reacting torques.

(d) The Calculation:

With the magnitude of the cylinder pressure, p_p, at a given crank angle θ and at a given engine speed being known, F_r and F_c were calculated by the above formulas, and F_p, F_s, F_a, F_t, F_b, R_x, R_y, G_x, G_y, etc. were obtained by graphical methods. Then with the forces being known and the dimensions of the crankshaft being measured, the stresses were calculated. (See Appendix E, an example of the calculation).

(e) The Curves:

The calculations were repeated for each crank angle and at several combinations of engine loads and engine speeds. The stresses were then plotted on curves against crank angles and engine speeds.

(f) The Natural Frequency of Torsional Vibration:

(See Appendix D).

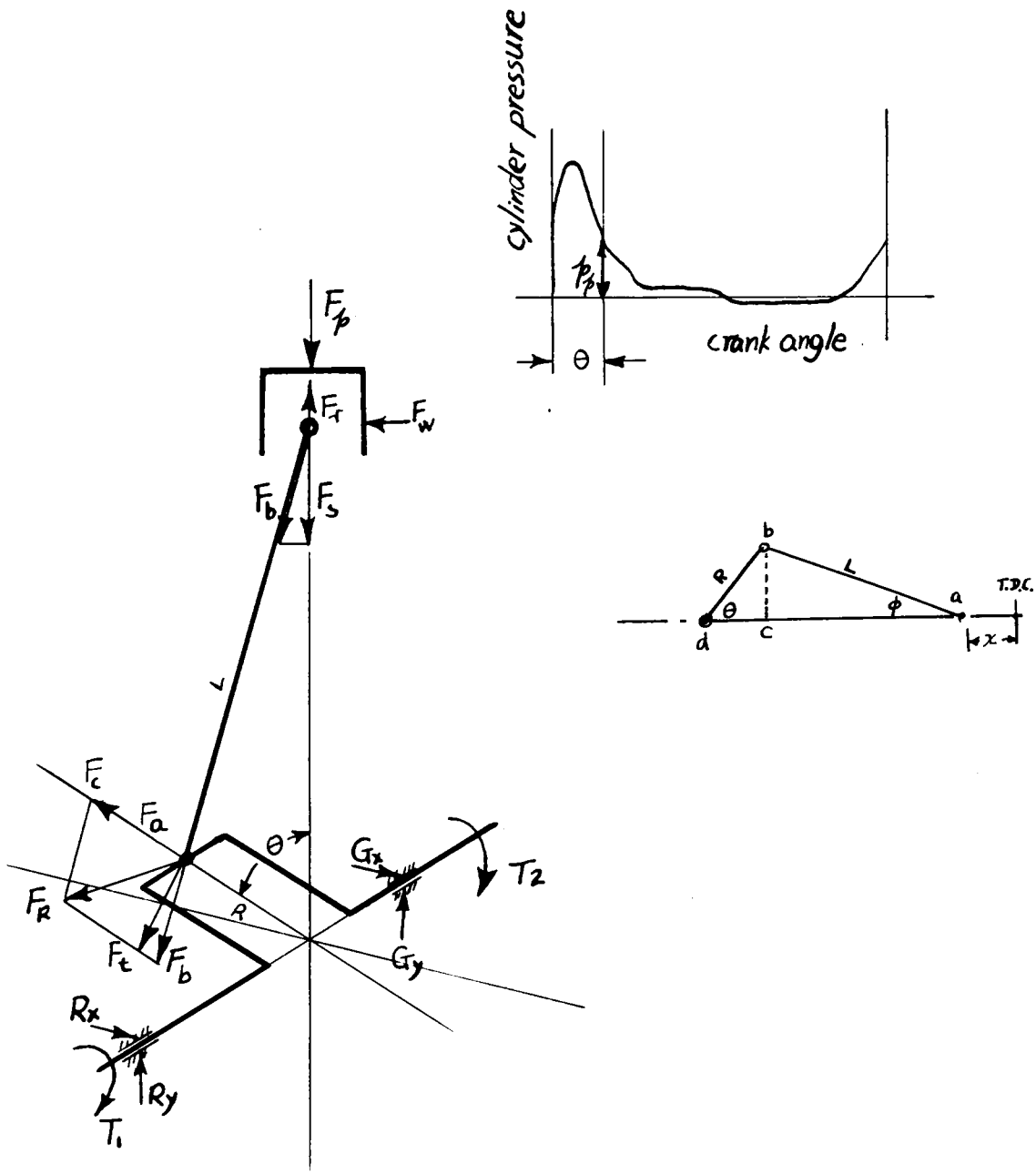

Fig.18 Schematic drawing showing the forces acting on the crankshaft of the engine.

C. Results

1. The experimental data:

The strain curves and the cylinder pressure curves are shown in Fig. 19 to Fig. 20. The conditions at which the curves were taken are given in the following.

Fig. 19(a) -- Cylinder pressure signal; engine was driven at 600 rpm; calibration setting 1/5.

Fig. 19(b) -- Torsional strain signal from strain gages located near the flywheel; engine was driven at 600 rpm; calibration setting 10.

Fig. 19(c) -- Cylinder pressure signal; engine was driven at 1200 rpm; calibration setting 1/5.

Fig. 19(d) -- Torsional strain signal from strain gages located near the flywheel; engine was driven at 1200 rpm; calibration setting 10.

Fig. 19(e) -- Cylinder pressure signal; engine was driven at 1800 rpm; calibration setting 1/5.

Fig. 19(f) -- Torsional strain signal from strain gage

located near the flywheel; engine was driven at 1800 rpm; calibration setting 10.

Fig. 19(g) -- Torsional strain signals from the gages located near the flywheel; engine was driven between 600 rpm and 1935 rpm.

Fig. 20(h) -- Same as Fig.19(g) except that the signals are more than a complete engine cycle.

Fig. 20(i) -- Tensile strain signal from strain gages located near the flywheel; engine was driven at 1290 rpm; calibration setting 10.

Fig. 20(j) -- Bending strain signal from the gages located near the flywheel; engine was driven at 1600 rpm; calibration setting 10.

Fig. 20(k) -- Tensile strain signal from strain gages located on the crankweb; engine was driven at 1800 rpm; calibration setting 1.

Fig. 20(l) -- Bending strain signal from gages located on the crankweb; engine was driven at 1935 rpm; calibration setting 2.

Fig. 20(m) -- Electrical disturbance caused by the

ignition unit on the strain gages located near the flywheel; engine ran at 2730 rpm; calibration setting 41.

Fig. 20(n) -- Torsional strain signal from strain gages located near the flywheel; engine ran at 2730 rpm; calibration setting 41.

It should be noticed that the signals were amplified at different rates when they were recorded; thus, the scales are not the same for all curves.

The scales of the curves were determined from the calibrating signals. The strain corresponding to the height of the deflection of the calibrating signal is

$$S = \frac{\text{(calibration factor)x(calibration setting)}}{\text{number of active arms in the bridge circuit}} \mu\text{in/in}$$

for example, the calibrating signal shown in Fig. 19 (b) has the following data:

Calibration factor = 58 (read from the chart on the Bridge-Amplifier)

Calibration setting = 10 (read from the Bridge-Amplifier)

Number of active arms = 4

Thus

$$S = \frac{58 \times 10}{4} = 145\ \mu\text{in/in} \qquad \text{where } \mu = 10^{-6}$$

The calibration signal had a deflection of six divisions; therefore, each division corresponding to a strain value of 24.2 μin/in.

The pressure scale was determined from a calibration curve which gave corresponding values between the pressure and the height of deflection of the calibration signals, (see Article 2.c.(1) page 46.). For example, the calibration signal in Fig. 19(a) has a deflection corresponding to a pressure of 140 lb./in.^{2} The deflection of the calibrating signal was three divisions high, thus each division corresponding to a pressure of 46.6 lb/in^2.

2. The reproduction of the experimental curves:

As previously mentioned in Article B. 2. page 61, the signals recorded from the instrument were combinations of the strain signal,or the pressure signal, and the noise. The true strain, or the pressure signal curve was obtained by drawing a fine line along the neutral axis of the noise wave.

After the noise was eliminated, the strain curves were enlarged and were transformed into stress curves by the relation that stress = strain x 30 x 10^6 (for steel).

3. The comparisons:

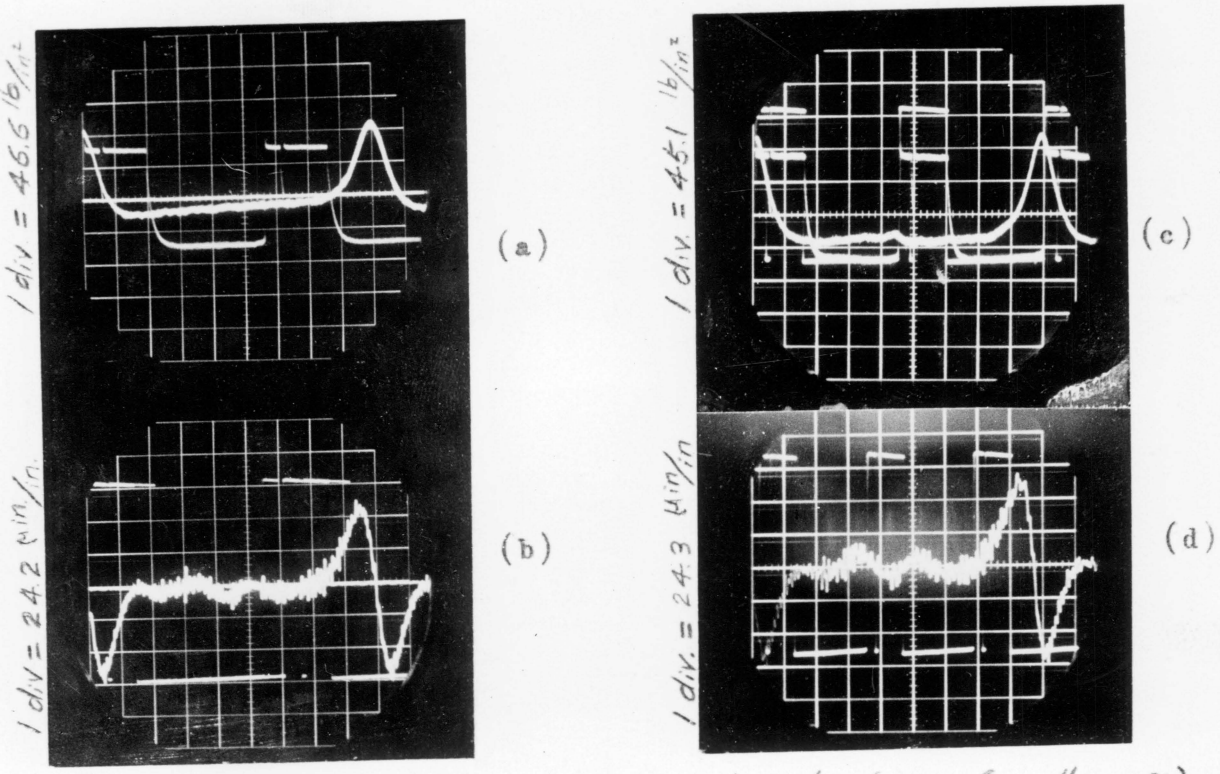

Scale of abscissa : 1 divison = 80° crank angles (same for all curves)

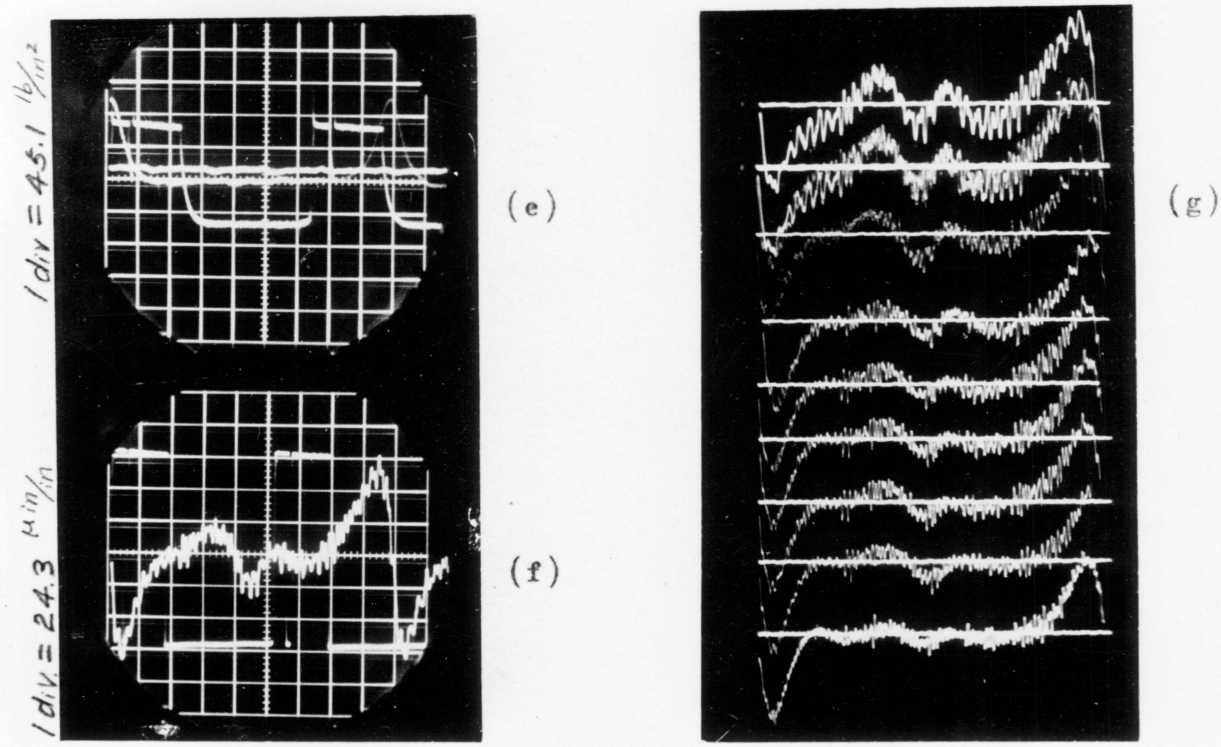

Fig.19 Experimental Data -- Strains and Pressure

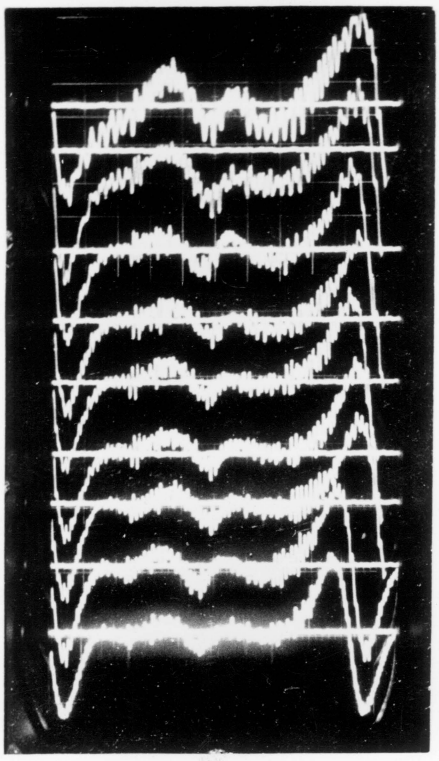

(h)

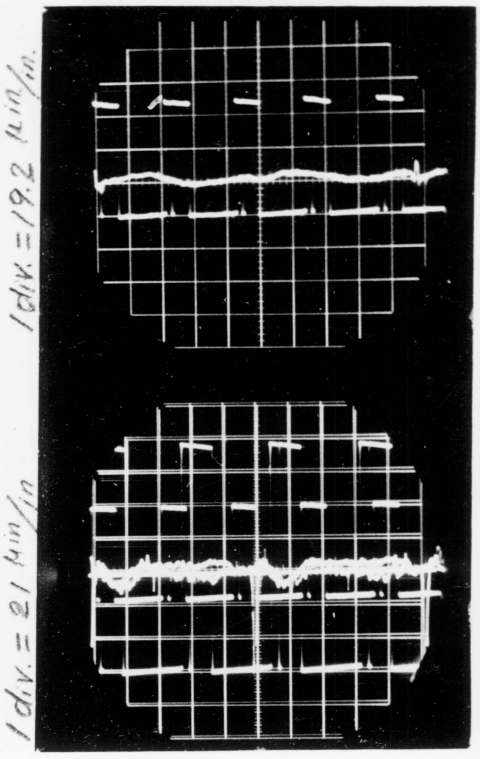

(i)

(j)

Scale of abscissa : 1 division = 80° crank angles (same for all curves)

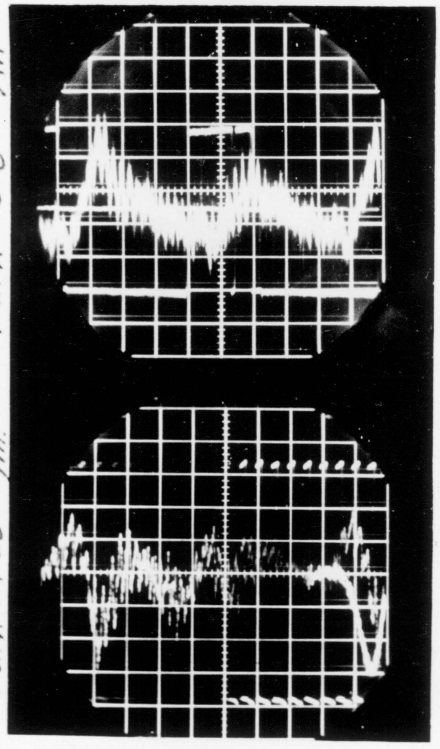

(k)

(l)

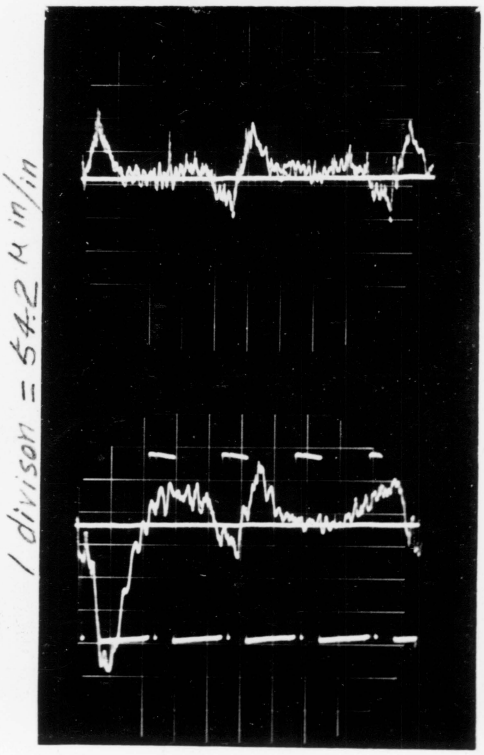

(m)

(n)

Fig.20 Experimantal Data -- strains and pressure

The graphical comparisons of the experimental curves with the analytical curves are shown in Fig. 21, Fig. 22, and Fig. 23.

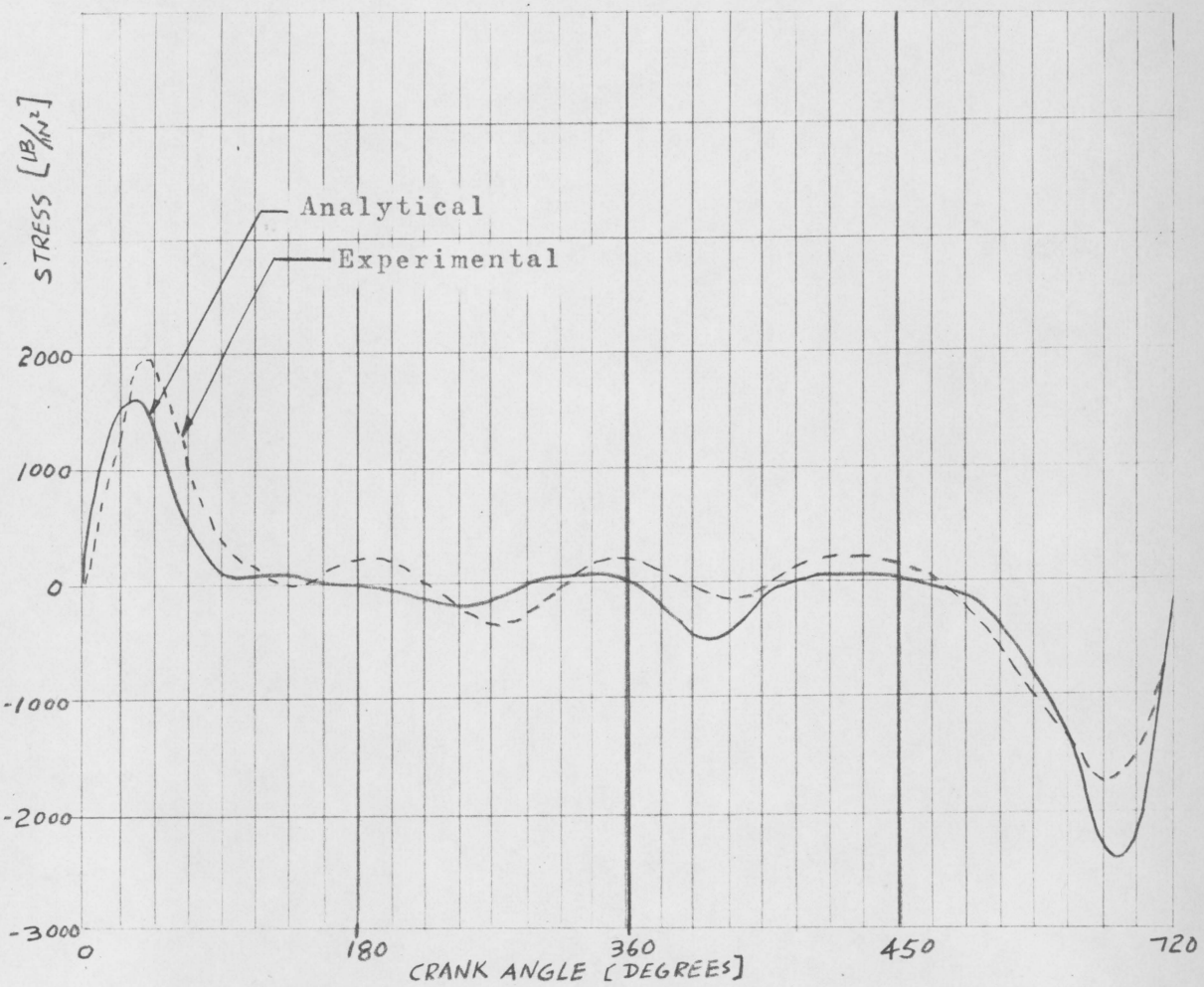

Condition: engine was driven at 1800 r.p.m.
Stress: stress due to torsional load
Location: on surface of the shaft near the flywheel
Direction of stress: 45° with axis of the shaft

Fig.21 The comparison of the analytical and experimental results

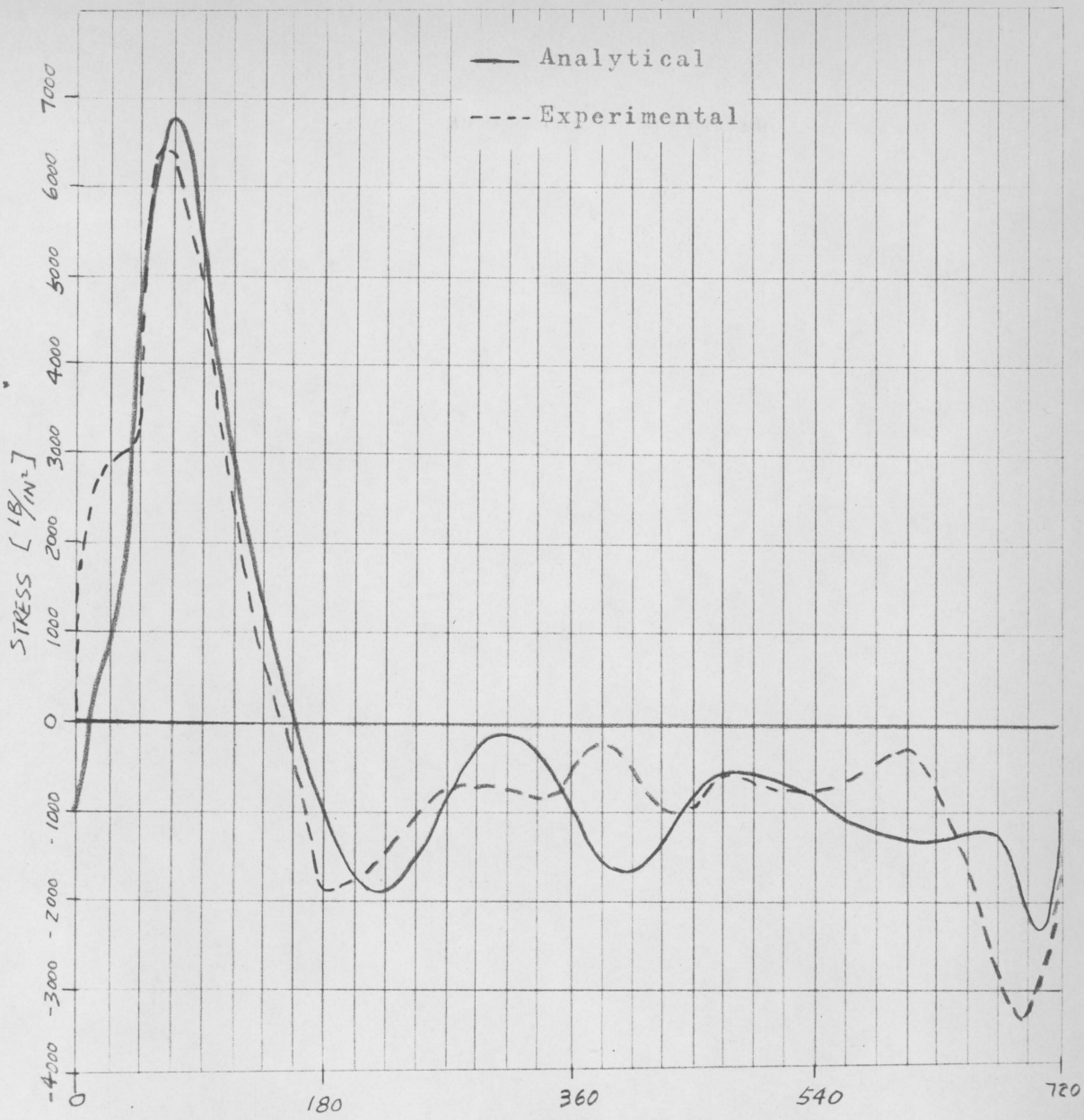

Condition: engine ran at 2730 rpm
Stress: stress due to torsional load
Location: on surface of the shaft near the flywheel
direction of stress: 45° with axis of the shaft

Fig. 22 The comparison of the analytical and experimental results

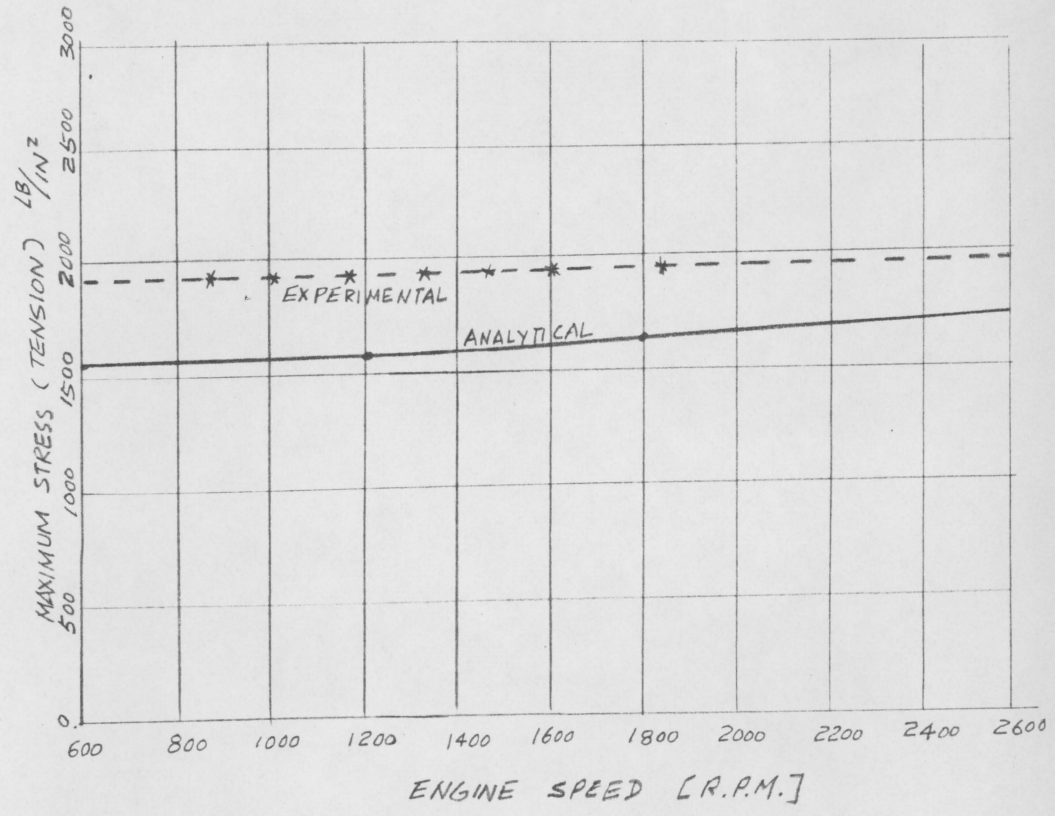

Condition: Engine was driven by the motor
Stresses: torsional stresses on surface of the shaft near the flywheel

Fig. 23 The comparison of the analytical and experimental results

IV THE DISCUSSION OF THE RESULTS

The result of the experimental part of the investigation was not as satisfactory as the writer had expected. This was due mainly to high electrical disturbances from various sources which make it impossible to obtained very accurate results while using small strain gages. The effects of electrical disturbances from the surroundings were reduced with proper grounding and shielding of the instruments. However, the electrical disturbances caused by the communicating devices between the rotating gages and the stationary instruments were at a comparatively high level. They influenced the results directly because the communicating devices were connected in series with the strain gages. Although these disturbance were brought down to a lower level by the development of a solid-to-liquid slip-ring unit, they could not be eliminated entirely. Furthermore, the strain gages located near the flywheel of the engine were subjected to a rotating electromagnetic field, and the extremely high voltage generated by the secondary coil of the ignition unit penetrated through the shields around the gages and the leads. All the attempts to eliminate this effect failed.

A possible way to reduce further the electrical disturbance is to use large strain gages on the crankshaft. This increases the strength of the signal, (or in other words, reduces the relative level of the disturbance), and would give better results. This is possible on a larger engine.

For the stresses on the surface of the shaft near the flywheel the graphical comparisons, (see Figs. 21 and 22), show that the experimental curves and the analytical curves compared favorably in magnitude and in the pattern. However, the analytical and the experimental stresses on the crankweb could not be compared. As shown in Fig. 20(k) and Fig. 20(l) no obvious trace of the strain signals from the gages on the crankweb could be obtained. This was due to the fact that the strength of the signal from the gages located at this section was lower than the strength of the electrical disturbance. According to the analytical method the stress at this portion of the crankweb was 230 lb./in.^{2} when the engine was driven by the generator, and 546 lb./in.^{2} when the engine ran under its own power and drove the generator. The equivalent resistance change in each gage was 1.92 milli-ohms and 4.48 milli-ohms respectively. The

electrical disturbances under these two conditions were equivalent to 3 milli-ohms and 9.8 milli-ohms, respectively.

According to the original plan, the natural frequency of torsional vibration of the crankshaft was to be determined experimentally by running the engine at a range of speed above and below the calculated resonance speed. However, the idea was abandoned later because the resonance speed was too high and could not be reached. The natural frequency calculated analytically was 57,800 rpm.

Some error was present in the experimental result because of the electrical disturbance, and in the analytical result because of the simplification of the method.

V. CONCLUSIONS

The following conclusions were drawn from the investigation:

1. It was possible to determine the stresses on the surface of the crankshaft of an internal combustion engine by means of electrical resistance strain gages.

2. The stresses calculated by the analytical method closely coincided in magnitude with the stresses determined experimentally, and the curves obtained by both methods were similar in their pattern.

3. The stress on the surface of the crankshaft near the flywheel was mainly due to the inertia of the flywheel. The magnitude of the stress depended upon the magnitude of the unbalanced torque between the input and the output torque and was only slightly influenced by the engine speed and the engine load.

VI. SUMMARY

The objective of this investigation dealt mostly with the experimental determination of the stresses on the surface of the crankshaft of an internal combustion engine. The experimental results were compared with the results obtained by an analytical method to determine the agreement between the two.

Stresses on the surface of the crankweb and on the surface of the shaft near the flywheel were investigated.

In the experimental method, the stresses were determined by the use of electrical resistance strain gages. The stresses induced on the crankshaft by torsional loads, bending loads, and axial thrust loads were determined separately.

Electrical communication between the rotating gages and the stationary recording instruments was provided by means of two slip-ring units. Two special slip-ring units employing the liquid to solid contact method were developed and used in the investigation.

The analytical determination of the stresses was carried out in a simplified way with the formulas which were generally used in the field of internal combustion engine design.

The graphical comparisons of the results are shown in Fig. 21, Fig. 22, and Fig. 23.

VII. RECOMMENDATIONS

With the experience gained in the investigation the following recommendations are suggested:

1. Since the slip-ring unit is a preferable device for maintaining electrical contacts between the rotating strain gages and the stationary instruments, strain gages with the highest possible gage factor and gage resistance to reduce the relative noise level of the slip-ring should be used.

2. The liquid to solid slip-ring unit which was developed and used in this investigation was recommended for only short periods of application. Further improvements such as the use of different materials for the housing, using a complete seal, etc., will be required if the unit is to be used for longer periods of investigation.

3. The etched foil strain gages are recommended for stress analysis on sharply curved surfaces; for example, the stress concentration on fillets. Strain gages of this type are extremely flexible and are much easier than the wire gages to apply on a curved surface.

4. A multi-channel recording instrument which can record several signals at the same time is preferable. However, if the instrument can only take one record at

a time, (such as the oscilloscope used in this investigation), a switch system should be used to save time and to assure correct connections.

VIII BIBLIOGRAPHY

1. Langer, B. F. " Design and Application of Magnetic Strain Gage ", Proceedings of the Socity for experimental Stress Analysis, Cambridge, Massachusetts, Volume I, No. 2, 1944, pp.82-89.
2. Dobie, W. B. " Electric Resistance Strain Gauges", The English Universities Press Limited, London, 1948, p.XI.
3. Walstrom F. Douglas " Measurement of Operating stresses in an Aircraft Engine Under Power ", National Advisory Committee for Aviation, Cleveland, Ohio, War Time Reports Series "E" No. 41 (ARR No. ESb01), 1945
4. Society of Automotive Engineers. War Engineering Board, " The Development of Improved Means for Evaluating Effects of Torsional Vibration on Internal Combustion Engine Installations ", Society of Automotive Engineers, Inc,, New York, 1945, p.467.
5. Hathaway, Claude N, " Electrical Instrument for Strain Analysis, Cambridge, Massachusetts, Volume I. No. 1, 1943, p.83.
6. Perry, C. C. and Lissner, H. R. " The strain Gage Primer", McGraw-Hill Book Company, New York, 1955.

7. Discussion following presentation of Mr. H. C. Roberts paper on Electrical Gaging Methods, Proceedings of the Society for Experimental Stress Analysis, Cambridge, Massachusetts, Volume II, No. 2, 1945, p. 101.

8. Tarbox, John " Selecting and Applying Wire Strain Gages", Machine Design, January 1955, p. 208.

9. Dutee, Francis J.; Phillips, Franklyn W.; and Kemp, Richard H. " National Advisory Committee for Aviation, Cleveland, Ohio, War Time Report, Series "E" No. 2, 1945.

10. Ormondroyd J."Problem of Torsional Vibration Increases with Engine Power", Machine Design, The Johnson Publishing Company, Cleveland, June, 1931, p. 37

11. " Torsional Vibrations Break Crankshafts ", Power, Volume 69, No. 9, Feburary 23, 1929, pp. 371 -373.

12. Society of Automotive Engineers War Engineering Board, " The Development of Improved Means for Evaluating Effects of Torsional Vibration on Internal Combustion Engine Installations ", Society of Automotive Engineers, Inc., New York, 1945, p 483.

13. Trent H. F. " A Comparison of the Forces in the Connecting Rod of an Internal Combustion Engine as Determined Experimentally and Analytically " Virginia Polytechnic Institute, Blacksburg, Virginia, 1958.

IX. ACKNOWLEDGMENTS

To

and , the writer wishes to express his sincere appreciation for the help and guidance received during the research and the writing of this thesis. The writer also wishes to thank , and the other members of the Mechanical Engineering Department for their interest and co-operation. All these persons, together, have made possible the successful completion of this project.

The writer wishes to thank the , , for their valuable information and their generosity in allowing the writer to share their paterns during the investigation of this project.

The writer also wishes to thank for her help received during the preparation of this thesis.

The vita has been removed from the scanned document

XI. APPENDICES

Appendix A

Specifications of the Engine[13]

Revolutions per minute ---------- 3,000

Horsepower ----------1.5

Compression ratio ---------- 5.5:1

Torque ----------2.6 ft-lb.

Number of cylinder ---------- 1

Bore ---------- 2 in.

Stroke ----------1.75 in.

Length of connecting rod, center to center -----3.125 in.

Radius of crank arm ---------- 0.875 in.

Weight of connecting rod ---------- 0.18 lb.

Weight of piston, complete with wrist pin, rings, etc. ---------- 0.31 lb.

Appendix B

Equations Used in Calculating Analytical Data

1. Piston position with respect to crank angle:

From Fig. 18

$$\overline{ac} = L \cos \phi$$

$$\overline{cd} = R \cos \theta$$

$$\overline{bc} = L \sin \phi = R \sin \theta$$

Since

$$x + \overline{ac} + \overline{cd} = L + R$$

$$x + L \cos \phi + R \cos \theta = L + R$$

or

$$x = L (1 - \cos \phi) + R (1 - \cos \theta) \text{ ---------(1)}$$

Because

$$L \sin \phi = R \sin \theta$$

$$\sin \phi = R \sin \theta / L$$

From basic trigonometric functions

$$\cos \phi = (1 - \sin^2 \theta)^{\frac{1}{2}}$$

Therefore

$$\cos \phi = (1 - R^2 \sin^2 \theta / L^2)^{\frac{1}{2}} \text{ ----------(2)}$$

By binomial theorem

$$(1 - R^2 \sin^2 \theta / L^2)^{\frac{1}{2}} = 1 + R^2 \sin^2 \theta / L^2 - R^4 \sin^4 \theta / 8L^4 + R^6 \sin^6 \theta / 16L^6 + \cdots\cdots\cdots$$

Since the values of sin θ and R/L are relatively small the terms $- R^4 \sin^4 \theta / 8L^4 + R^6 \sin^6 \theta / 16L^6 + \cdots\cdots$ can

be neglected without causing any appreciable error, then Eq.(2) becomes

$$\cos \phi = 1 + R^2 \sin^2\theta / 2L^2$$

substitute it into Eq.(1) to obtain

$$x = L \left(1 - 1 + R^2 \sin^2\theta / 2L^2 \right) + R \left(1 - \cos \theta \right)$$

or

$$x = R^2 \sin^2\theta / 2L + R \left(1 - \cos \theta \right) \quad \text{---------(3)}$$

From trigonometric functions

$$\cos 2\theta = \sin^2\theta - \cos^2\theta$$

$$= \sin^2\theta - \left(1 - \sin^2\theta \right)$$

$$= 2 \sin^2\theta - 1$$

or $\sin^2\theta = \frac{1}{2} \left(1 + \cos 2\theta \right)$

Eq.(3) becomes

$$x = R^2 \left(1 + \cos 2\theta \right)/4L + R \left(1 - \cos \theta \right) \quad \text{--(4)}$$

2. Velocity and acceleration of the piston:

From Eq.(4)

$$x = R^2 \left(1 + \cos 2\theta \right)/4L + R\left(1 - \cos \theta \right)$$

Since

$$V = \frac{dx}{dt} \quad \text{and}$$

$$\theta = \frac{2\pi N}{60} t$$

Where V = The instantaneous Velocity of the piston in inches per second

N = Angular speed of the crankshaft in revolution per minute

t = Time interval in seconds

if the engine runs at a constant speed, N is a constant, and

$$d\theta = 2\pi N\, dt/\, 60$$

or

$$d\theta/dt \quad 2\ N/60$$

$$V = \frac{dx}{dt} = \frac{dx}{d\theta}\cdot\frac{d\theta}{dt} = \frac{2\ N}{60}\cdot\frac{dx}{d\theta}$$

$$V = \frac{2\pi N}{60}\frac{d}{d\theta}\left[R^2\ (\ 1 + \cos\ 2\theta\ )/4L\ + R\ (\ 1 - \cos\theta)\right]$$

$$= \frac{2\pi N}{60}\left[\ -\frac{R^4}{4L}2\sin\ 2\theta - R\ \sin\ \theta\ \right]$$

or

$$V = \frac{2\pi N}{60}\left[R\ \sin\ \theta - R^2\sin\ 2\theta/2L\ \right] \text{----------(5)}$$

Let A be the instantaneous acceleration of the piston in inches per second

$$A = \frac{dV}{dt} = \frac{dV}{d\theta}\cdot\frac{d\theta}{dt} = \frac{dV}{d\theta}\cdot\frac{2\pi N}{60}$$

or

$$A = \frac{2\pi N}{60}\ x\ \frac{d}{d\theta}\ (\ R\ \sin\ \theta - R^2\sin\ 2\theta\ /\ 2L\ )$$

$$= \frac{2\pi N}{60}\ (\ R\ \cos\ \theta + \frac{R^2}{L}\ \cos\ 2\theta\ )\ \frac{2\pi N}{60}$$

or by further simplification

$$A = \frac{\pi^2 N^2 R}{900} \cos\theta + \frac{R}{L} \cos 2\theta \quad \text{----------(6)}$$

3. Inertia force due to reciprocating masses:

The reciprocating masses include the masses of the piston assembly and a equivalent mass of the connecting rod. Without inducing appreciable error, the equivalent reciprocating mass of the connecting rod is taken as the mass of the small end of the connecting rod.

Let W_r = the total masses in reciprocating motion. From basic dynamics

$F_r = W_r \, A / g$ Where F_r = the inertia force due to the reciprocating masses in pound.

A = the acceleration of the reciprocating masses in inches per second per second.

g = gravitational acceleration 386.4 inches/second/second.

Substitute Eq.(6) into the above equation to obtain

$$F_r = \frac{W_r}{g} \cdot \frac{\pi^2 N^2 R}{900} \left(\cos \theta + \frac{R}{L} \cos 2\theta \right)$$

With the following data:

W_r = 0.35 pound

L = the length of the connecting rod = 3.125 in.

R = radius of crank arm = 0.875 in.

N = crankshaft speed in r.p.m.

θ = crank angle in degree

$$F_r = 9.06 \times 10^{-6} \times N^2 \left(\cos \theta + 0.28 \cos 2\theta \right) \text{ -- (7)}$$

4. Inertia force due to the rotating motion of the big end of the connecting rod:

From basic dynamics the centrifugal force due to a rotating mass is given by the equation

$$F_c = \frac{W_c}{g} \left(\frac{2\pi N}{60} \right)^2 R$$

Where W_c = Weight of the big end of the connecting rod = 0.14 pound

g = 386.4 in./sec./sec.

R = radius of the crank arm = 0.875 in.

Subtituting the above known values in to the above equation to obtain

$$F_c = 3.48 \times 10^{-6} N^2 \text{ ----------(8)}$$

Appendix C

The property of the Wheatstone-Bridge Circuit

A Wheatstone-bridge circuit is shown in Fig. 24. From basic physics,

$$i_1 = \frac{V_{cd}}{R_1+R_2} \quad , \quad i_2 = \frac{V_{cd}}{R_3 + R_4}$$

$$V_{ca} = i_1 R_1 = \frac{R_1 V_{cd}}{R_1 + R_2}$$

$$V_{cb} = i_2 R_4 = \frac{R_4 V_{cd}}{R_4 + R_3}$$

$$V_{ab} = V_{ca} - V_{cb} = \frac{R_1 V_{cd}}{R_1 + R_2} - \frac{R_4 V_{cd}}{R_4 + R_3}$$

$$= V_{cd} \left(\frac{R_1}{R_1 + R_2} - \frac{R_4}{R_4 + R_3} \right)$$

$$= E \left[\frac{R_1 R_3 - R_4 R_2}{(R_1 + R_2)(R_4 + R_3)} \right] \qquad \text{----------(9)}$$

Where $V_{cd} = E$

If, at the begining, the bridge circuit is balanced and the resistances $R_1 = R_2 = R_3 = R_4 = R$,

$V_{ab} = 0$

Let R_1, R_2, R_3, and R_4 represent the resistance of the strain gages 1, 2, 3, and 4. Then, since the four gages have the same gage resistance when they are not under strain, $R_1 = R_2 = R_3 = R_4 = R$, and $V_{ab} = 0$.

When the strain gages are under a load, the resistances of the gages are changed, let the final resistance be:

$R_1 = R + \Delta R_1$

$R_2 = R + \Delta R_2$

$R_3 = R + \Delta R_3$

$R_4 = R + \Delta R_4$

From Eq.(9)

$$V_{ab} = E \left[\frac{(R + \Delta R_1)(R + \Delta R_3) - (R + \Delta R_4)(R + \Delta R_2)}{(R + \Delta R_1 + R + \Delta R_2)(R + \Delta R_4 + R + \Delta R_3)} \right]$$

$$E \frac{R(R_1 - R_3 - R_2 - R_4) - R_1 R_3 - R_2 R_4}{(2R - R_1 - R_2)(2R - R_4 - R_3)} \quad \text{---(10)}$$

The following cases are considered:

Case 1. All the four arms have the same resistance changes.

$\Delta R_1 = \Delta R_2 = \Delta R_3 = \Delta R_4$

$$V_{ab} = E \left[\frac{R(0) + 0}{(2R + \Delta R_1 + \Delta R_2)(2R + R_4 + R_3)} \right] = 0$$

The bridge remains balanced.

Case 2. Both the adjacent arms have the same resistance changes

$\Delta R_1 = \Delta R_2$ and $\Delta R_3 = \Delta R_4$ or $\Delta R_1 = \Delta R_4$ and $\Delta R_2 = \Delta R_3$

$$V_{ab} = E\left[\frac{R(0) + 0}{(2R + \Delta R_1 + \Delta R_2)(2R + \Delta R_4 + \Delta R_3)}\right] = 0$$

The bridge remains balanced.

Case 3. All the arms have the same magnitude of resistance change but in different directions

$\Delta R_1 = -\Delta R_4$

$\Delta R_3 = -\Delta R_2$

$\Delta R_1 = \Delta R_3$

$\Delta R_2 = \Delta R_4$

From Eq. (10)

$$V_{ab} = E\left[\frac{R(\Delta R_1 + \Delta R_1 + \Delta R_1 + \Delta R_1) + \Delta R_1 \Delta R_1 - \Delta R_1 \Delta R_1}{(2R + \Delta R_1 - \Delta R_1)(2R + \Delta R_4 - \Delta R_4)}\right]$$

$$E = \frac{4R\Delta R_1}{4R^2}$$

$$E = \frac{\Delta R_1}{R}$$

An unbalanced voltage occurs across the bridge circuit, and the unbalanced voltage is proportional to the resistance change in the strain gage.

If now the strain gages 1, 2, 3, and 4 are cemented to a circular shaft and the shaft is put under the forces as shown in Fig. 25, the resistance of each gage is changed.

The resistance change are dependent upon the strains on the surface of the shaft at which the gages are located.

As shown in the Fig. 25 the forces are composed of a torque, a bending moment, and an axial thrust force. The effect of each of the loads on the resistance changes in the gages is considered separately as follow:

1. The torque force --- When the shaft is twisted by a torque,

Gage 1 is extended and $R_1 = R + \Delta R_{t1}$

Gage 2 is compressed and $R_2 = R + \Delta R_{t2}$

Gage 3 is extended and $R_3 = R + \Delta R_{t3}$

Gage 4 is compressed and $R_4 = R + \Delta R_{t4}$

Since the gages are under the same magnitude of strain and have the same gage factor, $\Delta R_{t1} = \Delta R_{t2} = \Delta R_{t3} = \Delta R_{t4}$, and this condition is the same as the Case 3 as previously described. Therefore, an unbalanced voltage $V_{ab} = E \frac{\Delta R_t}{R}$ occurs.

2. The bending moment --- When the shaft is bent as shown in Fig. 25,

Gages 1 and 2 are compressed $R_1 = R - \Delta R_{b1}$

$R_2 = R - \Delta R_{b2}$

Gages 3 and 4 are extended $R_3 = R + \Delta R_{b3}$

$R_4 = R + \Delta R_{b4}$

Also since $|\Delta R_{b1}| = |\Delta R_{b2}| = |\Delta R_{b3}| = |\Delta R_{b4}|$, this condition

is equivalent to Case 2 as previously described and the circuit remains in balance.

C. The axial thrust --- When the shaft is compressed or extended by an axial force, all the gages have the same decrease or increase in their resistance. This condition coincides with Case 1 and thus no unbalanced voltage occurs.

Conclusion: With the strain gages connected in the Wheatstone-bridge as shown in Figs. 24 and 25, the bridge circuit is only sensitive to the torsional load.

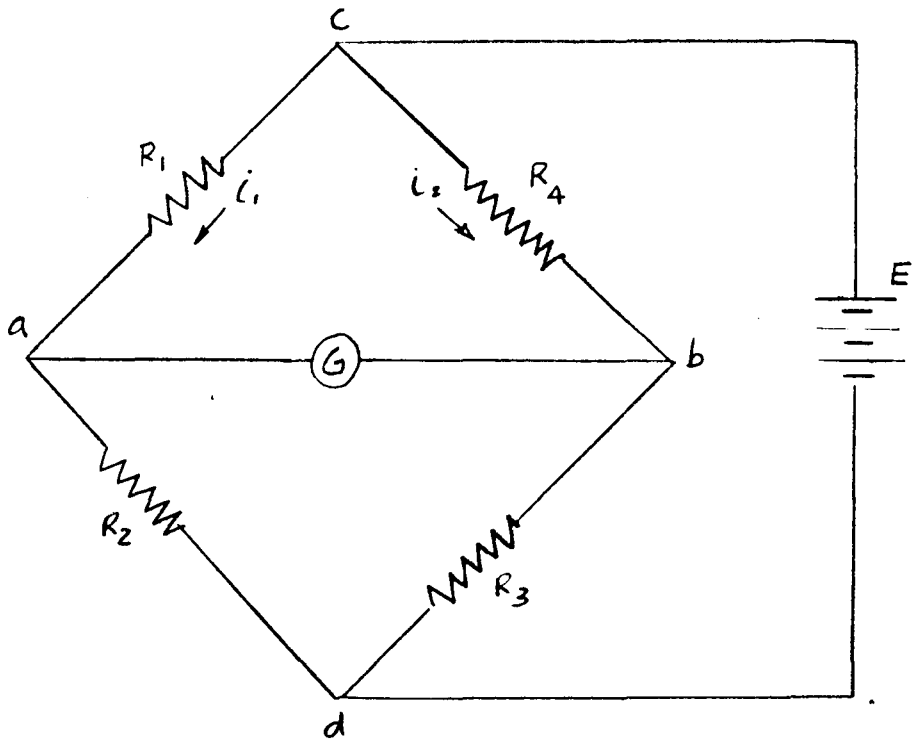

FIG 24 THE WHEATSTONE - BRIDGE

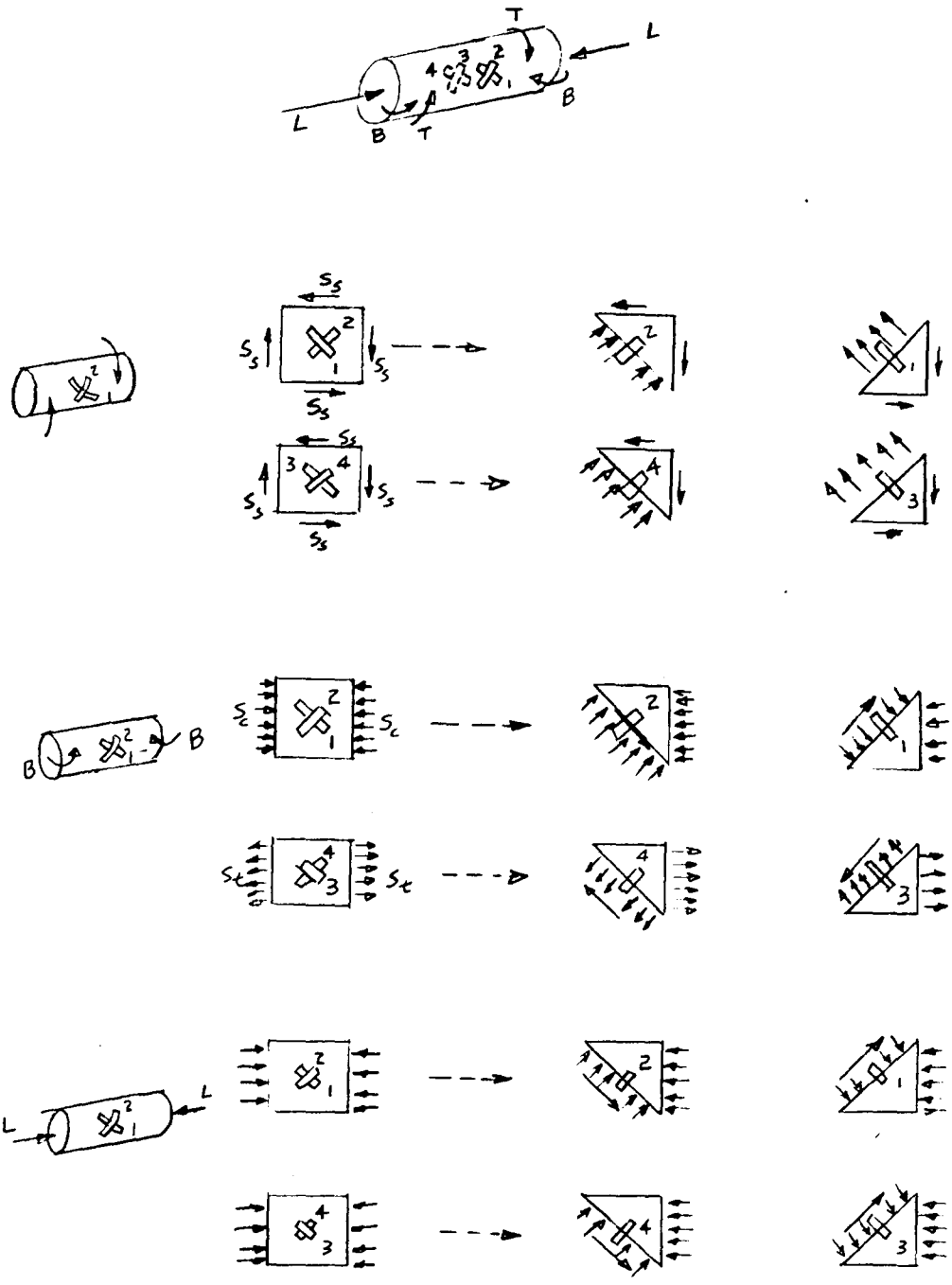

FIG 25 The strains on the surface of a circular shaft

Appendix D

The Natural Frequency of Torsional Vibration of the Crankshaft

1. The moment of inertia of each component of the crankshaft system:

	Moment of inertia ($\times 10^{-5}$) lb.-in.-sec^2
1. pully	393.00
2. camshaft	121.00
3. gear on crankshaft	8.94
4. journal (right end)	2.64
5. crankweb and balancing weight (right)	102.27
6. crank pin	23.70
7. big end of the connecting rod	27.80
8. piston and small end of connecting rod	34.60
9. crankweb and balancing weight (left)	99.81
10. journal (left)	2.14
11. cam (on crankshaft)	3.60
12. shaft	1.52
13. flywheel	7260.60
14. starting gear	33.13
15. slip-ring attachment	2.54

B. Inertia of the equivalent system, (see Fig. 26):

$I_1 = \frac{1}{4}(1) + \frac{1}{4}(2) + (3) + \frac{1}{2}(4) = 138.3 \times 10^{-5}$ lb.-in.-sec^2

$I_2 = \frac{1}{2}(4) + (5) + (6) + (7) + (8) + (9) + \frac{1}{2}(10) + \frac{1}{2}(11)$

$= 292.4 \times 10^{-5}$ lb.-in.-sec.^{2}

$I_3 = \frac{1}{2}(10) + \frac{1}{2}(11) + (12) + (13) + (14) + (15)$

$= 7298.5 \times 10^{-5}$ lb.-in.-sec.^{2}

C. The length of the shaft of the equivalent system:

The crankshaft was reduced to an equivalent shaft of one inch in diameter as shown in Fig. 26.

D. The natural frequency:

The natural frequency was determined by the following equations:

$$(I_1\beta_1 + I_2\beta_2 + I_3\beta_3)\,\omega^2 = 0$$

$$\beta_2 = \beta_1 - \frac{I_1\omega^2\beta_1}{k\ t_1}$$

$$\beta_3 = \beta_2 - \frac{I_1\omega^2\beta_1 - I_2\omega^2\beta_2}{k\ t_2}$$

Where β is the maximum relative angular deformation in radians

ω is the natural frequency of torsional vibration in radians per second.

I is the inertia in lb.-in.-sec.^{2}

k_t is the torsional spring constant of the shaft in lb.-in/radian

$$k_{t1} = \frac{\pi d^4 G}{32 L_1}$$

$$= \frac{\pi (1)^4 x 12 x 10^6}{32 \times 5.21} = 2.26 \times 10^5$$

$$k_{t2} = \frac{\pi (1)^4 \times 12 \times 10^6}{32 x\ 7.275} = 1.62 \times 10^5$$

Where d = diameter of the equivalent shaft [in.]

G = a constant 12×10^6 [lb/in^2]

L = the length of the equivalent shaft [in.]

The natural frequency is determined by tabulation as shown in Fig. 26. The solution is

$\omega = 6051$ [radians/second]

The lowest natural frequency of torsional vibration is

$$N = \frac{60\omega}{2\pi} = \frac{60 \times 6051}{2\pi} = 57,800 \text{ rpm.}$$

The first order of resonance occurs at

2N = 115,600 rpm.

ω = 6000 radians/sec

I	$I\omega^2$	β	$I\omega^2\beta$	$\Sigma I\omega^2\beta$	k_t	$\frac{1}{k_t}\Sigma I\omega^2\beta$
138.3×10^{-5}	4.97×10^4	1	4.97×10^4	4.97×10^4	2.26×10^5	0.22
292.4×10^{-5}	10.5×10^4	0.78	8.2×10^4	13.17×10^4	1.62×10^5	0.812
7298.5×10^{-5}	263×10^4	-0.032	-8.41×10^4	6.66×10^4		

ω = 6200 radians/sec

I	$I\omega^2$	β	$I\omega^2\beta$	$\Sigma I\omega^2\beta$	k_t	$\frac{1}{k_t}\Sigma I\omega^2\beta$
138.3×10^{-5}	5.3×10^4	1	5.3×10^4	5.3×10^4	2.26×10^5	0.234
292.4×10^{-5}	11.2×10^4	0.766	8.6×10^4	13.9×10^4	1.62×10^5	0.859
7298.5×10^{-5}	280×10^4	-0.093	-26×10^4	-12.1×10^4		

ω = 6050 radians/sec

I	$I\omega^2$	β	$I\omega^2\beta$	$\Sigma I\omega^2\beta$	k_t	$\frac{1}{k_t}\Sigma I\omega^2\beta$
138.3×10^{-5}	5.06×10^4	1	5.06×10^4	5.06×10^4	2.26×10^5	0.225
292.4×10^{-5}	10.7×10^4	0.776	8.3×10^4	13.36×10^4	1.62×10^5	0.826
7298.5×10^{-5}	265×10^4	-0.05	-13.25×10^4	$+0.11\times10^4$		

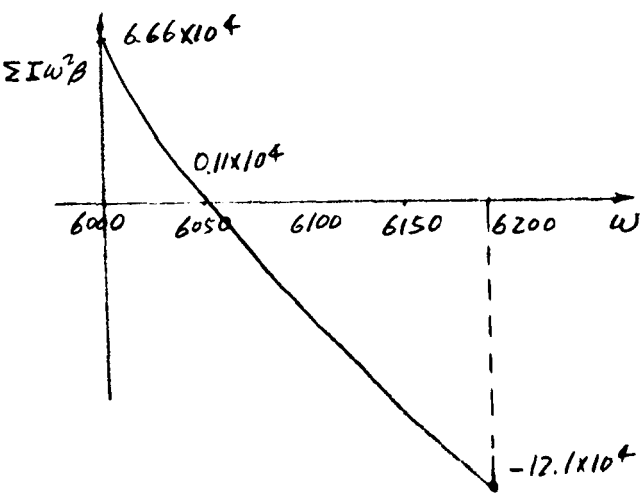

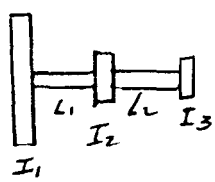

Fig 26 The determination of the natural frequency of torsional vibration

Appendix E

An Example of the Analytical Method

1. Data

   Engine specification -- Given in Appendix A

   Engine speed --- 1800 rpm. (driven by the generator)

   Cylinder pressure --- Given in Fig. 27

   Cross sectional area of the crankweb (cut across at the center of the strain gages) ---- 0.846 in^2

   Diameter of the shaft at which the gages were located ------- 11/16 in.

2. Equations:

   Inertia force of the reciprocating masses

   $$F_r = 9.02 \times 10^{-6} x N^2 (\cos \theta + 0.28 \cos 2\theta) \quad -- (7)$$

   Inertia forces of the big end of the connecting rod

   $$F_c = 3.48 \times N^2 \times 10^{-6} \quad ---------- (8)$$

3. Procedure and Solutions:

   (a) <u>The gas pressure force:</u>

   The cylinder pressure at each crank angle, θ, is given in Fig. 27. Since the total force acting on the top of the piston is

   $$F_p = \frac{\pi}{4} (\text{bore})^2 \times P_p = \frac{\pi}{4} (2)^2 \times p_p = \pi P_p$$

   the F_p vs. θ curve is thus obtained from the p_p vs. θ curve by changing the original scale to a new scale.

Original scale: 1 in. = 38.1 lb/in^2

New scale: 1 in. = 38.1 x π = 122.5 lb.

(b) <u>The inertia force of the piston and the small end of the connecting rod:</u>

From Eq.(7) the inertia force of the reciprocating masses is

$$F_r = 9.02 \times 10^{-6} \times 1800^2 (\cos \theta + 0.28 \cos 2\theta)$$

$$= 2.91 (\cos \theta + 0.28 \cos 2\theta) \text{ lb.}$$

F_r can be calculated from the equation for each value of θ or can be obtained by the graphical method as shown in Fig.28. F_r was then plotted against θ

(c) <u>The resultant force of F_p and F_r:</u>

F_p and F_r are combined to obtain F_s by the graphical method.

(d) The force acting along the axis of the connecting rod:

The force F_s is separated into two forces F_b and F_w by the graphical method as shown in Fig.18. F_b is the force acting along the axis of the connecting rod.

(e) <u>The inertia force of the big end of the connecting rod:</u>

From Eq.(8), the inertia force is

$F_c = 3.48 \times 10^{-6} \times 1800^2 = 11.28$ lb.

(f) The forces acting on the crank pin:

As shown in Fig. 18, the forces F_b and F_c are combined to obtain F_R. Then, F_R is separated into a tangential force F_t and an axial force F_b. The procedure was repeated for each crank angle θ, and then F_t and F_b were plotted in curves against θ. The same scale is used for all the force vectors and the force coordinates.

(g) The stresses on the surface of the crankweb:

The stresses at the area at which the strain gages were located are caused by the forces shown in Fig. 29. Let F_b be the inertia force due to the masses of the crank pin and the masses of the upper part of the webs.

$$F_d = \frac{0.141}{32.2}\left(\frac{2\times1800}{60}\right) \times 0.875 = 11.5 \text{ lb.}$$

The forces F_b and F_d are assumed to be equally divided and taken by the two webs. The axial load on each web is than equal to

$$F_w = \tfrac{1}{2}\left(F_b + F_d\right)$$

The F_w vs. θ curve is obtained from the F_b vs. θ curve by reducing the force scale to one half of

the original scale and by moving the zero-axis by an amount equal to F_d.

The stress caused by the force F_w is

$$S_w = F_w / A$$
$$= F_w / 0.846$$

The S_w vs. θ curve is then obtained from the F_w vs. θ curve by changing the force scale into a stress scale. The stress scale is

$$1 \text{ in.} = \frac{122.5}{0.846 \times 2} = 72.5 \text{ lb/in}^2$$

The stress due to the bending moment (caused by the force F_t) is equal to

$$S_t = 6M/bh^2$$
$$= 6T_1/0.74\ (1.13)^2$$
$$= 6.34\ T_1$$

Where M = Bending moment = $T_1 = F_t \times 0.875$

b = thickness of the crankweb = 0.74 in.

h = width of the crankweb = 1.13 in.

The S_t vs. θ curve is obtained from the T_1 vs. θ curve by changing the force scale to a stress scale. The stress scale is

$$1 \text{ in.} = 6.34 \times 122.5 \times 0.875 = 680 \text{ lb/in}^2$$

The crankwebs are also subjected to bending moment and the torque as shown in Fig. 29, but the strain gages were located at the neutral plan of the

bending moment and the torque and thus are not sensitive to these loads.

(h) The stresses on the shaft near the flywheel:

The torque imposed on this section of the shaft is a part of the driving torque. From Fig. 18

$F_t \times R = T = T_1 - T_2$

According to the assumption that the torque T_1 is a constant at a given speed and load of the engine, the T_2 vs. θ curve has the same pattern as the F_t vs. θ curve since R is also a constant. When the engine drives the generator, the torque T_1 is equal to the mean torque because the flywheel does not consume any power. When the engine was driven by the generator, T_1 equals to zero since no power is generated or consumed by the gas in the cylinder of the engine, (the pumping work is negligible), and therefore $T_2 = T$

The T vs. θ curve is obtained from the F_t vs. θ curve by changing the force scale to a torque scale. The torque scale is

1 in. = 122.5 x 0.875 = 107 in.-lb.

The T_2 vs. θ curve is the same as the T vs. θ curve when the engine is driven by the generator.

When the engine drives the generator, the T_2 vs. θ curve is obtained from the T vs. θ curve by moving

up the zero-axis by an amount equal to the mean torque T_1.

The shear stress due to the torque T_2 is equal to

$$S_s = 16\ T_2/\pi d^3 = 15.7\ T_2$$

Where d = diameter of the shaft

= 11/16 in.

The S_s vs. θ curve is obtained from the T_2 vs. θ curve by changing the torque scale to a stress scale. The stress scale is

1 in. = 107 x 15.7 = 1680 lb/in^2

The principle stress on the surface of the shaft due to a pure torsional load is equal in magnitude to the shear stress and is at a 45° angle from the axis of the shaft.

The stress due to the axial load and bending load is zero since no axial force and bending moment are acting on the shaft.

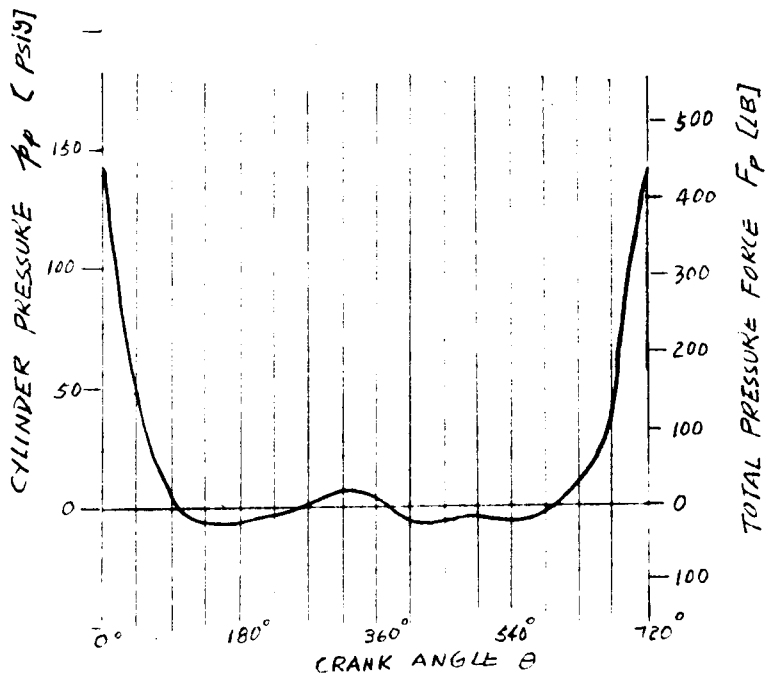

FIG. 27 Cylinder pressure and total pressure force

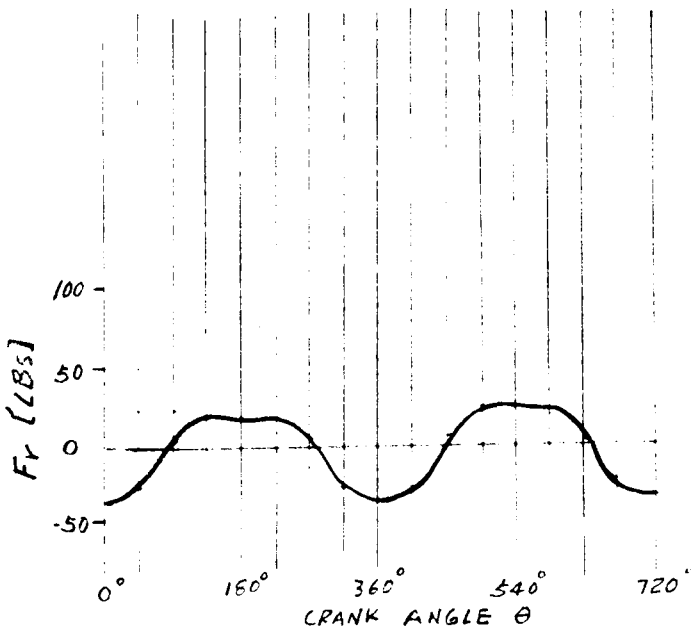

FIG. 28 The inertia force of the reciprocating masses

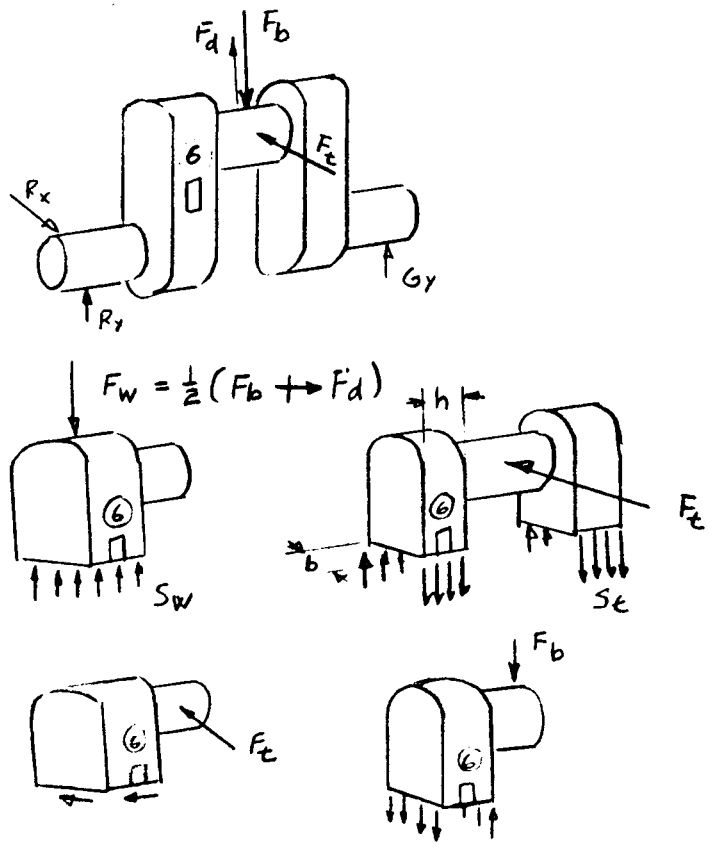

FIG 29 The forces and the stresses in the crankweb

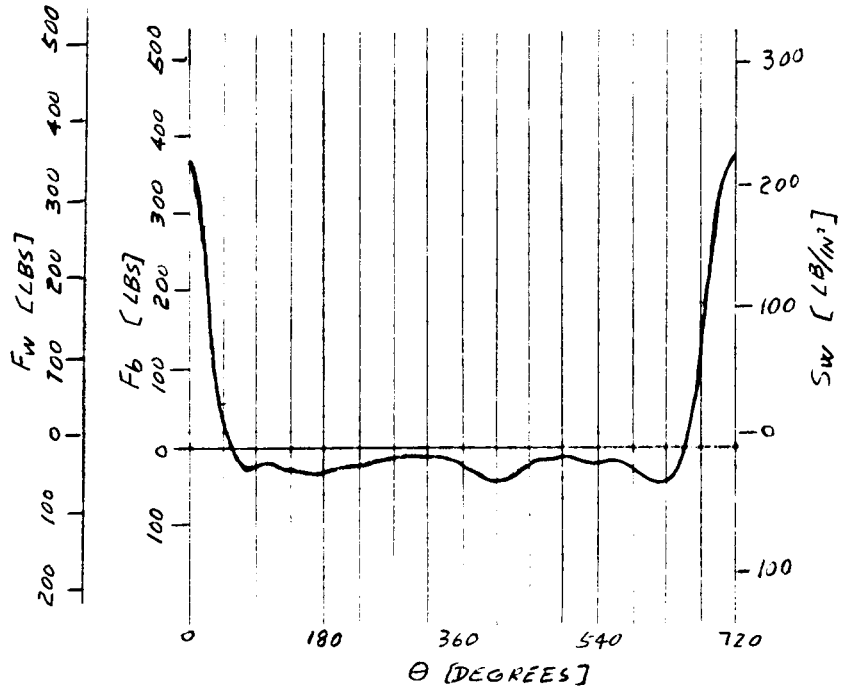

FIG 30 The axial force and stresses in the crankweb

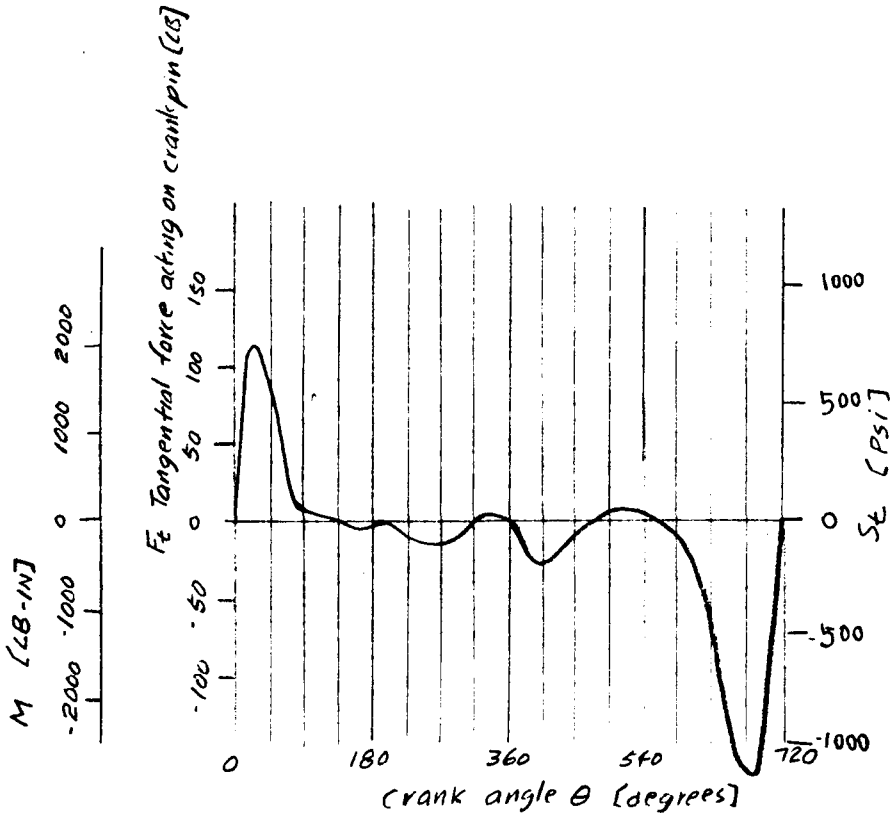

FIG.31 The bending force and the stress on the crankweb

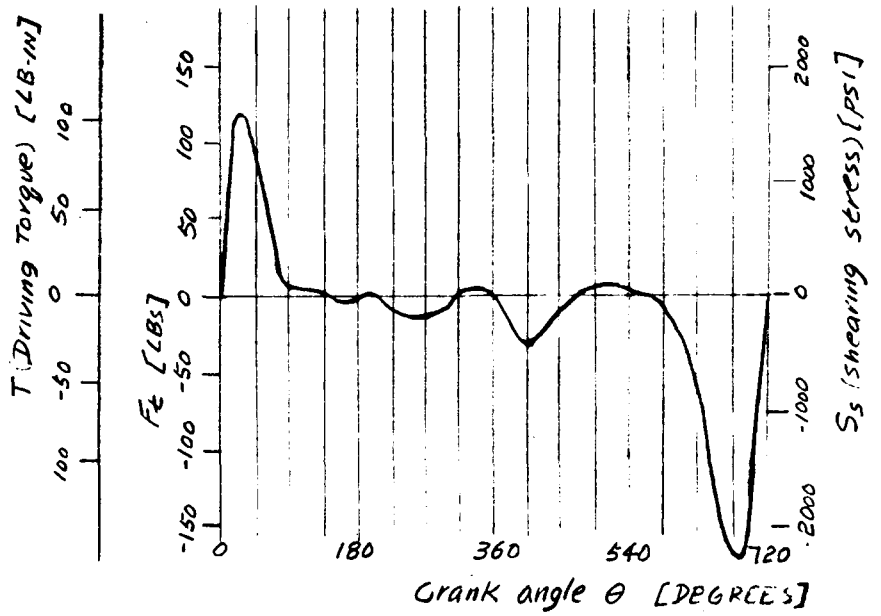

FIG. 32 The forces and stresses on the crankshaft (near the flywheel)

ABSTRACT

In order to study the degree of accuracy with which the analytical methods used in crankshaft design would predict the actual operating stresses in the crankshaft of an internal combustion engine, electrical resistance strain gages were applied to the accessible parts of the crankshaft of a single cylinder gasoline engine to sense the actural operating strains. From the recorded strains the operating stresses were determined and were compared to the analytically determined stresses.

Oscilloscope and camera were used as the indicating and recording instruments while simplified formulas were used in the calculations. Stresses at various engine speeds and engine loads were determined by both methods and were plotted in curves against engine speeds and crank angles.

In the graphical comparisons the stresses determined by using electrical resistance strain gages agreed well with the stresses obtained analytically.